e-**X**tra*

Plant growth promotion driven by a novel *Caulobacter* strain

Dexian Luo,[1,2] Sarah Langendries,[1,2] Sonia Garcia Mendez,[1,2,3] Joren De Ryck,[1,2] Derui Liu,[1,2] Stien Beirinckx,[1,2,4] Anne Willems,[3] Eugenia Russinova,[1,2] Jane Debode,[4] and Sofie Goormachtig[1,2,†]

[1]Department of Plant Biotechnology and Bioinformatics, Ghent University, 9052 Ghent, Belgium; [2]Center for Plant Systems Biology, VIB, 9052 Ghent, Belgium; [3]Department of Biochemistry and Microbiology, Faculty of Sciences, Ghent University, 9000 Ghent, Belgium; [4]Plant Sciences Unit, Flanders Research Institute for Agriculture, Fisheries and Food (ILVO), Burg. Van Gansberghelaan 96, 9820 Merelbeke, Belgium

†Corresponding author: Sofie Goormachtig; E-mail: sogoo@psb.vib-ugent.be

*The *e*-**X**tra logo stands for “electronic extra” and indicates that seven supplementary figures are published online.

ABSTRACT

Soil microbial communities hold great potential for sustainable and ecologically compatible agriculture. Although numerous plant-beneficial bacterial strains from a wide range of taxonomic groups have been reported, very little evidence is available on the plant-beneficial role of bacteria from the genus *Caulobacter*. Here, the mode of action of a *Caulobacter* strain, designated RHG1, which had originally been identified through a microbial screen for plant growth-promoting (PGP) bacteria in maize (*Zea mays*) is investigated in *Arabidopsis thaliana*. RHG1 colonized both roots and shoots of *Arabidopsis*, promoted lateral root formation in the root, and increased leaf number and leaf size in the shoot. The genome of RHG1 was sequenced and was utilized to look for PGP factors. Our data revealed that the bacterial production of nitric oxide, auxins, cytokinins, or 1-aminocyclopropane-1-carboxylate deaminase as PGP factors could be excluded. However, the analysis of brassinosteroid mutants suggests that an unknown PGP mechanism is involved that impinges directly or indirectly on the pathway of this growth hormone.

Plant roots are associated with a wide variety of bacteria from different taxonomic groups, many of which can enhance plant growth and/or stress tolerance via diverse mechanisms, including hormone modulation (Tsukanova et al. 2017), nutrient uptake enhancement (Richardson et al. 2009; Van Deynze et al. 2018), or disease suppression (Berendsen et al. 2018; Kwak et al. 2018). These bacteria, referred to as plant growth-promoting rhizobacteria (PGPR) (Vacheron et al. 2013), have received increasing attention, because they provide a sustainable and ecological solution for the agricultural challenges we are facing (Gouda et al. 2018; Toju et al. 2018).

As phytohormones control plant growth and its interaction with the environment, PGPR have been proposed to affect the plant hormonal landscape for their establishment in or around the plant roots and for the growth stimulation. Indeed, PGPR have been shown to be able to generate phytohormones, such as auxins and cytokinins, or enzymes or compounds that interfere with the endogenous phytohormone production or with signaling pathways. For instance, *Azospirillum brasilense* Sp245 is an auxin-producing PGPR strain that promotes lateral root formation and enhances the expression of auxin-responsive genes in *Arabidopsis thaliana*. Both effects are impaired in the auxin biosynthesis mutant strain FAJ0009 (Spaepen et al. 2014). Also cytokinins that play an essential role in cell division and influence many aspects of plant growth and development (Schaller et al. 2014) have been shown to be produced by PGPR, such as *Bacillus* (Liu et al. 2013) and *Pseudomonas* (Pallai et al. 2012). Additionally, 1-aminocyclopropane-1-carboxylate (ACC) deaminase-producing PGPR, such as *Pseudomonas putida* UW4 (Hontzeas et al. 2004), modulate the plant ethylene levels by degrading the plant-generated ACC, thereby mitigating the plant

growth-inhibitory effects of ethylene (Glick 2014). On the other hand, PGPR have been found to regulate plant hormonal homeostasis without production of the respective hormones. For example, the volatile indole emitted by the rhizobacterium *Proteus vulgaris* JBLS202 enhances *Arabidopsis* growth through an interplay between the auxin, cytokinin, and brassinosteroid pathways (Bhattacharyya et al. 2015). Another example is the *Pseudomonas* model strain *P. simiae* WCS417, of which the auxin-producing ability had not been detected by either colorimetric assays in bacterial cultures or genome analysis (Zamioudis et al. 2013; Berendsen et al. 2015). However, both the induction of the PGP effect and expression of the induced systemic resistance (ISR) markers by this rhizobacterium depend on auxin signaling in *Arabidopsis* (Zamioudis et al. 2013; Stringlis et al. 2018). The early transcriptional response of *Arabidopsis* roots to this bacterium has a strong auxin signature (Stringlis et al. 2018), but the bacterial factor(s) responsible for this response remain(s) unknown.

Nitric oxide (NO), another key signaling molecule involved in diverse plant developmental processes and stress responses, is generated by bacteria and proposed to be a phytostimulating signal (Sami et al. 2018). In bacteria, NO production is mainly mediated by two types of nitrite reductase (Nir): the haem-cytochrome *cd*1 type encoded by *nirS* genes and the copper-containing type encoded by *nirK* genes (Zumft 1997). The *A. brasilense* strain Sp245 possesses two copies of the *NirK* gene (Pothier et al. 2008) and this strain generates NO on tomato (*Solanum lycopersicum*) roots (Creus et al. 2005). The *Azospirillum*-induced lateral root formation was blocked by the NO scavenger 2-(4-Carboxyphenyl)-4,4,5,5-tetramethylimidazoline-1-oxyl-3-oxide (CPTIO), hinting at the involvement of NO in this process (Creus et al. 2005). Correspondingly, the

Pseudomonas kilonensis F113-mediated modification of the root system architecture was significantly impaired in the *NirS* gene deletion mutant (Vacheron et al. 2018).

Next-generation sequencing analysis revealed that many more bacterial genera live in root endospheres and rhizospheres than previously anticipated (Bai et al. 2015; Fitzpatrick et al. 2018; Walters et al. 2018). Currently, for many of these genera, of which *Caulobacter* is one of them, no clues are supplied whether they contribute to plant growth or health. The *Caulobacter* genus has been frequently found in endospheres or rhizopheres of various plants grown in different soils (Bai et al. 2015; Fitzpatrick et al. 2018; Walters et al. 2018). Interestingly, the *Caulobacter* genus acts as one of the microbial "hubs" that are strongly interconnected and have a central impact on the leaf microbiome of *Arabidopsis* (Agler et al. 2016). Additionally, different *Caulobacter* strains have been isolated from diverse plants or rhizosphere soil, including *C. rhizosphaerae* 7F14^{T} from the rhizosphere soil of watermelon (*Citrullus lanatus*) (Sun et al. 2017), *C.* sp. HGR25 from horse gram [*Macrotyloma uniflorum* (Lam.) Verdc.] (Edulamudi et al. 2011), and *C. hibisci* THG-AG3.4^{T} from the rhizosphere of Mugunghwa flower (*Hibiscus syriacus* L.) (Moya et al. 2017), indicating that the association between *Caulobacter* and plants is ubiquitous in natural environments. However, little is known about the beneficial role of the *Caulobacter* members on plants.

Here we examine the *C.* sp. strain RHG1 that had been identified through a microbial screen for plant growth-promoting (PGP) endophytic bacteria in maize (*Zea mays*). The root colonization of the green fluorescent protein (GFP)-labeled strain was thoroughly analyzed in *Arabidopsis* by confocal microscopy. The PGP

effect was investigated by an in-depth growth analysis, the potential PGP traits in the RHG1 genome were examined, and concomitantly the impact on colonized plants was studied on *Arabidopsis* mutants and marker lines, affected in or representative for diverse hormone pathways, respectively.

RESULTS

RHG1 promotes plant growth in *Arabidopsis*.

The PGP effect of the *C.* sp. RHG1 in *Arabidopsis* was studied in an *in vitro* system, in which *Arabidopsis* seeds were inoculated with RHG1. Eighteen days after initiation of germination (DAIG), the fresh weights of both shoot and root had significantly increased after the bacterial inoculation (Fig. 1A and B).

As growth is a complex trait that integrates many different factors, among which are control of organ initiation, cell division, and cell expansion (Kalve et al. 2014), we examined how these factors could be influenced by the RHG1 inoculation. In the shoot, increase in both leaf size and total leaf number contributed to the enhancement of the shoot biomass of the inoculated plants (Fig. 1C and D). Furthermore, cellular analysis of the leaf epidermis revealed that the number of pavement cells, guard cells, and, accordingly, total epidermal cells was higher in plants inoculated with RHG1 than that of mock-treated plants (Fig. 2A to C). Interestingly, the pavement cells in the leaves of RHG1-inoculated plants were significantly smaller than those of mock-treated plants (Fig. 2D), suggesting that the enlargement in leaf size by RHG1 results from an increase in cell number instead of cell area. To assess the influence of RHG1 on root growth, we determined primary root length, lateral root number, lateral root density, and

total root length at 14 DAIG. RHG1 inoculation had a variable effect on the primary root length. The RHG1-inoculated plants had significantly shorter primary roots than the mock-treated roots in some of the experiments, but this phenotype was not stable in every experiment (Supplementary Fig. S1). However, in all the experiments, the impact of the RHG1 inoculation on the lateral root number, the lateral root density, and the total root length was consistent and positive (Fig. 1E to G), contributing to the increase in root biomass of the inoculated plants.

To evaluate whether the PGP effect of RHG1 was caused by the bacterial production of CO_2 or other easily diffusible volatile compounds, we used a cocultivation setup and tested whether the mock-treated plants grown besides the RHG1-inoculated plants in the same plate could benefit from the bacteria. In this setup, the fresh weight and lateral root number of the RHG1-inoculated plants were significantly higher than that of the mock-treated plants, but the increase in fresh weight and lateral root number by RHG1 in the cocultivation setup was not significantly different from that in plants grown in the setup in which the RHG1-inoculated and mock-treated plants were grown in different plates (Supplementary Fig. S2). This result suggested that the PGP effect of RHG1 is not caused by CO_2 or other easily diffusible volatile compounds.

Colonization pattern of RHG1 in *Arabidopsis*.

Next, we investigated whether RHG1 could enter the plant and live as an endophyte. The RHG1 colonization on *Arabidopsis* shoots and roots was determined by counting colony-forming units per milligram of fresh weight (CFU/mg FW). At 14 DAIG, the overall CFU/mg FW was in the range of 10^6 to 10^7 (average 8.81×10^6) or 10^6 to 10^8 (average 9.51×10^7) in the shoots or roots,

respectively. To examine the colonization pattern of RHG1 microscopically, we labeled RHG1 with GFP by means of the mini-Tn*5*--based transposon delivery system (Tombolini et al. 1997), which allowed the insertion of the GFP marker driven by a constitutive P*psbA* promoter into the chromosome of the bacteria. The resulting strain is referred to as RHG1::GFP hereafter. The shoot and root weights of plants inoculated with the RHG1::GFP strain were higher than those of the mock-treated control (Supplementary Fig. S3), but the fresh weights of the RHG1::GFP-inoculated and the RHG1-inoculated plants did not differ significantly (Supplementary Fig. S3), indicating that the insertion of the GFP marker into the genome did not disturb the interaction of the bacteria with the plants. Then we analyzed the colonization pattern of RHG1::GFP by using confocal microscopy. At 14 DAIG, colonization of RHG1::GFP was observed on the root and leaf surfaces (Fig. 3A to E). Additionally, at sites where lateral roots emerged, the GFP signal was visible in-between the plant cells (Fig. 3E). To improve the in-depth imaging within roots, we employed the ClearSee protocol (Kurihara et al. 2015) that fixes and clears the inoculated root with a mounting medium with high-refractive index that allows high light penetration. The microscopic observation of the cleared tissues confirmed the colonization by RHG1::GFP on the root surface and the intercellular positions at lateral root emergence (Fig. 3F to H), as seen via imaging of live specimens. Hence, RHG1 colonizes the root and leaf surfaces and enters the root at the lateral root bases, but without signs of colonization of the vascular tissues.

Genome and encoded functions of RHG1.

To test whether signs for root colonization and PGP traits could be found, we sequenced the RHG1 genome. The draft genome sequence was assembled with the Shovill platform. The total length of the RHG1 assembly was approximately 5.6 million base pairs (bp) with an average G+C content of 67.55%. This assembly was made up of 19 contigs, of which the largest is 861938 bp and the smallest 1000 bp. The N50 value is 643962 bp. The draft genome of RHG1 presented 5174 coding sequences, 63 transfer RNA genes, and 4 ribosomal RNA (rRNA) genes.

Additionally, the RHG1 strain was subjected to a phylogenomic analysis by comparing its genome against that of other 38 known strains of the genus *Caulobacter* and with three outgroups of the genus *Brevundimonas* as close relatives. The bcgTree software was utilized that evaluated 107 essential core genes found in most bacteria (mostly housekeeping and ribosomal proteins) (Ankenbrand and Keller 2016). Interestingly, RHG1 occurred in a clade with 15 other *Caulobacter* strains, including *C. vibrioides* (OR37, CB13b1a, CB2^T [formerly known as the type strain of *C. crescentus*], DSM 9893^T, CB15, NA1000, and CB1), *C. segnis* (ATCC 21756^T), and some unspecified strains (*C*. sp. FWC2, *C.* sp. OV484, *C*. sp. Root342, *C*. sp. Root343, *C*. sp. X, *C*. sp. BP25, and *C*. sp. FWC26) (Supplementary Fig. S4). Remarkably, RHG1 is the most peripheral in the group, clearly separated from all the other strains in this clade (Supplementary Fig. S4), suggesting that RHG1 is evolutionarily distant when compared to other known *Caulobacter* species. To support these results, the similarity between RHG1 and the other strains was calculated by means of OrthoANIu (Yoon et al. 2017). The obtained values ranged from 72.02% to 84.58% Average Nucleotide Identity (ANI), with the highest values with *C.* sp.

OV484 (84.58% ANI), *C.* sp. Root342 (84.57% ANI), *C.* sp. Root343 (84.57% ANI), and *C.* sp. FWC2 (84.36% ANI). These results are consistent with the outcome of the bcgTree software, corroborating the observed evolutionary distance. As the genome sequences are not available for all the 11 validly named *Caulobacter* species, the 16S rRNA genes available for all the type strains were used to construct a maximum likelihood tree (Supplementary Fig. S5). In agreement with the results obtained in the phylogenomic analysis, RHG1 formed a separate lineage and its closest neighbors were *C. vibrioides* and *C. segnis* (Supplementary Fig. S5).

Special attention was given to the occurrence of genes linked to endophytic lifestyles (Mitter et al. 2013) and PGP functions (Lemanceau et al. 2017) (Table 1). Plant polymer-degrading enzymes (polysaccharide lyase and glycosyl hydrolases families) and reactive oxygen species (ROS)-detoxifying enzymes (catalase, peroxidase, superoxide dismutase), which have been proposed to be important for endophytic lifestyles (Mitter et al. 2013), were found as well as genes involved in flagellar motility and chemotaxis, which are key during the rhizosphere colonization. No genes occurred involved in ACC degradation (ACC deaminase) or auxin (such as tryptophan monooxygenase and indole-3-pyruvate decarboxylase), cytokinin (isopentenyl transferase), gibberellin (gibberellin 20-oxidase), or abscisic acid (isopentenyl-pyrophosphate isomerase and farnesyl diphosphate synthase) biosynthesis, nor genes involved in biocontrol activity (2,4-diacetylphloroglucinol [DAPG] biosynthesis and cyanhidric acid biosynthesis) or in biofertilization (phosphate solubilization and nitrogen fixation). Interestingly, a NirK protein, as well as other proteins involved in the

denitrification process (NO reductase and NO-responding transcriptional activator NnrR) were predicted from the genome of RHG1.

The nitrite reductase gene *nirK* of RHG1 is not crucial for its PGP trait.

The *nirK* gene present in the genome of RHG1 shows high similarity to known *nirK* genes from other bacteria, including *A. brasilense* Sp245 (Supplementary Fig. S6), which has been proposed to induce lateral root formation in tomato by the generation of NO (Creus et al. 2005; Pothier et al. 2008). This hypothesis raised the question whether the *nirK* gene-mediated NO production by RHG1 would contribute to its PGP function. Therefore, we tested whether deletion of *nirK* from the RHG1 genome might reduce the PGP effect of the bacterium. The *nirK* deletion mutant, referred to as RHG1 △*nirK* hereafter, was constructed through a recombination-based method (see Materials and Methods). The impact was analyzed of the RHG1 △*nirK* inoculation on lateral root number, lateral root density, and shoot and root weights of *Arabidopsis*. In comparison to the wild-type RHG1 strain, the plant growth parameters did not differ significantly (Fig. 4), suggesting that the *nirK* gene is not essential for the PGP function of RHG1.

Plant auxin, cytokinin, and ethylene signaling pathways are upregulated upon RHG1 inoculation, but probably not essential for the PGP effect.

Bacterial production of auxins, cytokinins, or ACC deaminase is frequently found to be a PGP trait in PGPR. Pathways or genes responsible for the generation of these compounds did not occur in the draft RHG1 genome. However, these pathways can also be modulated by currently unknown bacterial

compounds or enzymes. To rule out this hypothesis, we examined the responses of the plant hormone reporter lines to the RHG1 inoculation and assessed the PGP effect on the corresponding hormone mutant and transgenic lines. The expression of the auxin-responsive reporter *DR5:GUS* (Ulmasov et al. 1997) was upregulated by RHG1 in the shoot, but not in the root (Fig. 5A). Consistently, the expression of *DR5:GFP* was not significantly altered by the bacteria in the root (Fig. 5A). The auxin mutant and transgenic lines *yucca1D*, *35S:iaaL,* and *tir1afb2/3* were tested for RHG1-mediated PGP effect. *yucca1D* is an indole-3-acetic acid (IAA)-overproducing gain-of-function mutant (Zhao et al. 2001); the *35S:iaaL* line overexpresses the bacterial IAA lysine synthase that inactivates IAA (Jensen et al. 1998); *tir1afb2/3* is an auxin signaling mutant deficient in the auxin receptors TIR1, AFB2, and AFB3 (Dharmasiri et al. 2005). Total fresh weight of the plant, instead of separate shoot or root weights, was measured, because the weight of *35S:iaaL* and *tir1afb2/3* root was smaller than the minimum range of the analytic balance. The increase in plant fresh weight caused by RHG1 was not reduced in any of the auxin mutants or transgenic lines when compared to the *Arabidopsis* wild-type Columbia-0 (Col-0) (Fig. 5B).

Similarly, the cytokinin-responsive reporter *pARR5:GUS* (D'Agostino et al. 2000) was slightly upregulated by the bacteria in the shoot, but not in the root (Fig. 6A). However, RHG1 significantly promoted growth in terms of fresh root and shoot weights in the *ahk2/3/4* triple mutant, which is impaired in cytokinin signaling due to mutations in the cytokinin receptors AHK2, AHK3, and AHK4 (Nishimura et al. 2004) (Fig. 6B).

The expression of the ethylene-responsive marker *pEBS:GUS* (Stepanova et al. 2007) was upregulated both in the shoot and root in the RHG1-inoculated

plants when compared to the mock-treated control (Fig. 6C). Hence, we also tested whether the ethylene signaling pathway is required for the PGP effect. In the ethylene-insensitive mutant *ein2-5*, which is deficient in ethylene signal transduction due to a null mutation in the *ETHYLENE INSENSITIVE2* (*EIN2*) gene (Wang et al. 2007), the RHG1-mediated increase in plant weight was not attenuated when compared to the *Arabidopsis* wild-type Col-0 (Fig. 6D). Collectively, although the expression of the markers responsive to auxin, cytokinin, and ethylene were slightly upregulated upon RHG1 inoculation, none of the corresponding mutant or transgenic lines had a reduced PGP effect, indicating that these hormones do not play a main role in the observed PGP effect.

Brassinosteroid biosynthesis and signaling are required for the plant growth promotion by RHG1.

As brassinosteroids are essential phytohormones that regulate cell division, cell expansion, and plant growth (Saini et al. 2015), we wondered whether they were required for the PGP impact of RHG1. So, we tested their effect on the *constitutive photomorphogenesis and dwarfism* (*cpd*) (Szekeres et al. 1996) and *brassinosteroid-insensitive 1* (*bri1*) (Jaillais et al. 2011) mutants, which are deficient in brassinosteroid biosynthesis and signaling, respectively. Because of the sterility of both the homozygous *cpd* and *bri1* plants, the 5-day-old seedlings were inoculated, allowing the selection of homozygous mutants from the heterozygous population. At 14 DPI, the total plant fresh weight was determined, without division into shoot and root weights due to the small size of the mutants. In all the four independent replicates, the fresh weight of the wild-

type plants was increased by 20% to 53% upon inoculation with RGH1, but this effect was lessened in both the *cpd* and *bri1* mutants, although the different replicates varied (Fig. 7A; Supplementary Fig. S7). In three of the four replicates, the fresh weights of mock-treated and RHG1-inoculated *cpd* plants did not differ significantly, whereas only in one replicate the fresh weight of the RGH1-inoculated *cpd* plants had increased by 8%, a value significantly smaller than that of 20% in the wild type (Fig. 7A; Supplementary Fig. S7). Similarly, the plant fresh weight did not increase by RHG1 inoculation in the *bri1* mutant in three of the four replicates, except for one of the replicates, in which a smaller increase in the *bri1* mutant than that in the wild type was observed (15% and 53%, respectively) (Fig. 7A; Supplementary Fig. S7). These results indicate that brassinosteroid biosynthesis and signaling are necessary for the PGP effect of RHG1. Next, we analyzed whether brassinosteroid signaling was modulated by RHG1. BRI1-EMS-Suppressor 1 (BES1), a master transcription factor of brassinosteroid signaling, is phosphorylated, and inactivated in the absence of brassinosteroids. Upon brassinosteroid signaling activation, BES1 is dephosphorylated and triggered to regulate the downstream target genes (Yin et al. 2002; Saini et al. 2015). To examine the brassinosteroid signaling level upon RHG1 inoculation, the ratio between dephosphorylated and total BES1 proteins was assessed at 4 DPI, instead of 14 DPI, because the activation of the growth-triggering molecular signaling takes place before the PGP effects are observed. Additionally, the upregulation of the auxin, cytokinin, and ethylene markers were visible at 4 DPI, indicating that the interaction between the plants and the bacteria had been established at this time point. The dephosphorylation status of the BES1 proteins did not differ significantly between the mock-treated and RHG1-inoclulated plants

(Fig. 7B), implying that the bacterium did not modify directly the brassinosteroid signaling, although it was required for its PGP effect.

DISCUSSION

A growing list of PGPR, from a wide variety of genera, such as *Azospirillium*, *Bacillus*, *Azotobacter*, *Burkholderia*, and *Pseudomonas*, has been discovered in the past decades (Gouda et al. 2018). Nevertheless, identification of new PGPR strains, especially those with novel or improved PGP functions, is still of great value, because it will expand our understanding on the functional diversity of PGPR and allow us to exploit the full potential of PGPR for an ameliorated agriculture. The genus *Caulobacter*, with *C. vibrioides* as an important model system, has been well studied as model organism for the regulation of the bacterial cell cycle, asymmetric cell division, and cellular differentiation (Woldemeskel and Goley, 2017). Although bacteria of the *Caulobacter* genus have been isolated from the endosphere and rhizosphere of several plants, to our knowledge, RHG1 is the first *Caulobacter* strain for which the PGP function has been investigated in detail. The results from the genome comparison and the 16S rRNA gene sequence analysis indicate that this strain might represent a new species, but, because only one single strain is available, we cannot propose a formal description yet. In *Arabidopsis*, the RHG1 inoculation promoted the growth of both shoots and roots, with a leaf number, leaf size, shoot weight, lateral root number, total root length, and root weight higher in the inoculated plants than those in the mock control plants. Cellular analysis revealed that the RHG1 inoculation increased the number of leaf epidermal cells, but

decreased the cell area, suggesting that RHG1 enhances plant growth by promoting cell division. It is unclear whether the PGP factor is initially perceived by the shoot or the root or both, because in *Arabidopsis* both are colonized by RHG1.

It is fascinating to uncover the mechanisms that mediate the PGP function of RHG1. As the mock-treated plants did not benefit from the bacteria applied on the inoculated plants in the cocultivation setup, the PGP effect of RHG1 is probably not caused by easily diffusible volatiles that cause plant growth promotion by other PGPR (Kanchiswamy et al. 2015). The presence of a *nirK* gene in the genome of RHG1 prompted us to test whether the *nirK*-mediated NO production contributed to the PGP function of RHG1. However, the PGP effect by RHG1 was not reduced by the *nirK* gene deletion, suggesting that *nirK* is not crucial, in contrast to *A. brasilense* Sp245 (Creus et al. 2005). Hence, although both bacteria enhance the lateral root density, they seem to function through different mechanisms.

Modulation of the plant hormone landscape is another manner by which PGPR increase the root and shoot biomasses (Tsukanova et al. 2017). The bacterial genome analysis revealed that RHG1 probably lack genes encoding proteins involved in the bacterial production of auxins, cytokinins, or ACC deaminase, all well-known PGP markers. Nevertheless, the expression of the auxin-responsive marker *DR5:GUS* and the cytokinin-responsive marker *pARR5:GUS* was slightly upregulated in the shoot upon inoculation with RHG1. Besides the bacterial production of these hormones, some bacteria are known to regulate the plant hormone homeostasis by affecting the expression of plant genes involved in hormone biosynthesis or transport. For example, *Bacillus* sp.

LZR216 induces the expression of the auxin biosynthesis genes *NIT1*, *TAA1,* and *YUCCA1* and decreases the expression of the auxin transporters *AUX1*, *PIN1*, *PIN2*, and *PIN3* in *Arabidopsis* (Wang et al. 2015), whereas *Bacillus subtilis* SYST2 enhances the expression of the cytokinin biosynthesis gene *SlCKX1* in tomato plants (Tahir et al. 2017). However, given that the RHG1-mediated increase in plant weights was not attenuated in the *yucca1D*, *35S:iaaL*, *tir1afb2/3*, and *ahk2/3/4* mutants, the observed increase in marker gene expression is possibly indirectly caused by changes in other pathways rather than by the early perception of the bacteria. Interestingly, the upregulation of the *DR5* expression in response to RHG1 inoculation occurred in shoots, but not in roots, in contrast to *P. simiae* WCS417 that strongly activated the expression of *DR5:YFP* in roots and depended on auxin signaling for its PGP activity (Zamioudis et al. 2013). Hence, auxin might play a different role during the plant interactions with these two bacterial strains. Ethylene is a key regulator of the plant immune system and plays a crucial role in the regulation of the rhizobacteria-mediated ISR by PGPR, including *P. simiae* WCS417 (Pieterse et al. 1998, 2014). The expression of the ethylene-responsive marker *pEBS:GUS* was enhanced in both shoots and roots by RHG1. Thus, it would be interesting to test whether RHG1 might have an ISR effect when the host plants are challenged with pathogens.

What could the PGP factor of RHG1 be? The RHG1-mediated increase in fresh weight is dramatically lower in the brassinosteroid biosynthesis mutant *cpd* and the signaling mutant *bri1* than that in the wild-type plant, implying that the brassinosteroid pathway is required for the PGP effect. Nevertheless, the fact that the dephosphorylated level of the BES1 protein is not altered by RHG1 at 4 DPI suggests that the brassinosteroid signaling is not modified by RHG1, but

could possibly be temporarily activated by RHG1, while remaining undetected at the time point of the experiment. Hence, it will be valuable to further pinpoint how the RHG1 treatment and the brassinosteroids are interconnected.

Thus, the molecular mechanism underlying the PGP function of RHG1 is notwithstanding an intriguing question, because the RHG1-produced PGP factors that are perceived by plants and induce plant growth are still unknown. In this study, we ruled out the possibility of bacterially produced auxins, cytokinins, ACC deaminase, and NO as PGP factors, but we did not find any other genes/pathways encoding potential PGP factors in the draft genome of RHG1. Therefore, the PGP traits of RHG1 might be mediated by novel genes and mechanisms, because we are only just starting to comprehend the biology of soil microorganism communities and are still far away from understanding all their gene functions. For instance, 30% to 50% of the gene sequences available in public databases still lack functional annotations as of 2017 (Sévin et al. 2017). Therefore, it is of the high interest to investigate the mechanism underlying the PGP function of RHG1 in the future. For this purpose, forward genetic *in planta* screen for the identification of PGP traits of RHG1 will be applied.

MATERIALS AND METHODS

Plant materials and bacterial strains.

Arabidopsis thaliana (L.) Heynh. accession Col-0 and mutant and transgenic lines in the Col-0 background were used. Mutant and transgenic lines have been described previously: *DR5:GUS* (Ulmasov et al. 1997); *DR5:GFP* (Benková et al. 2003); *yucca1D* (Zhao et al. 2001); *35S:iaaL* (Jensen et al. 1998);

tir1afb2/3 (Dharmasiri et al. 2005); *pARR5:GUS* (D'Agostino et al. 2000); *ahk2/3/4* (Nishimura et al. 2004); *pEBS:GUS* (Stepanova et al. 2007); *ein2-5* (Wang et al. 2007); *bri1* (Jaillais et al. 2011); and *cpd* (Szekeres et al. 1996).

The *C.* sp. strain RHG1 was isolated from surface-sterilized roots of the maize variety LG30270 grown in agricultural field soil (50°58'41" N, 3°46'47.28"O; Merelbeke, Belgium). The GFP-labeled strain RHG1::GFP and the *nirK* gene deletion strain RHG1 △*nirK* were constructed in this study.

Plant inoculation and growth conditions.

Caulobacter strains, including the wild-type strain RHG1, the labeled strain RHG1::GFP, and the mutant strain RHG1 △*nirK*, were routinely grown in R2A medium (Reasoner and Geldreich, 1985) at 28°C. The bacterial inoculum was made by subculturing 1 ml of overnight culture in 15 ml fresh R2A medium for 3 h. Cells were collected by centrifugation for 5 min at 3000*g*, washed once, and resuspended in phosphate buffered saline (PBS) solution. The bacterial concentration was adjusted to OD_{600} = 0.1 (10^7 CFU/ml) and further diluted 10- or 1000-fold for seedling or seed inoculation, respectively. For seed inoculation, seeds were surface sterilized with chlorine gas and five seeds were sown per square Petri plate (120 mm × 120 mm) with half-strength Murashige and Skoog (MS) medium and 0.8% (w/v) agar. Subsequently, 1 µl PBS solution or bacterial inoculum was applied on each seed for mock treatment or bacterial inoculation, whereafter the plates were kept at 4°C in the dark for 2 days to synchronize seed germination and then placed vertically in the growth chamber. For seedling inoculation, seeds were sown and allowed to germinate under the same conditions. Four-day-old seedlings (or otherwise specified) were transferred to

fresh half-strength MS agar plates and inoculated by pipetting 8 µl PBS solution or bacterial inoculum onto the shoot and root of each seedling. After inoculation, all plants were grown vertically in a growth chamber at 21°C with a 16-h light/8-h dark photoperiod.

Measurement of the root architecture and plant weight parameters.

For the measurement of the root architecture parameters, images of Petri plates with *Arabidopsis* seedlings were captured by means of an EPSON Expression 11000XL A3 scanner. The lateral root number was counted manually. The root length was measured with the NeuronJ plugin of the ImageJ software. The fresh shoot and root mass were weighted by separating the seedlings at the shoot-root junction. Excised shoots and roots were quickly cleaned with paper tissues to remove the surface water and bacteria and immediately weighted on an analytical balance with a 0.1 mg resolution.

Enumeration of bacterial colonization.

Arabidopsis seeds were inoculated with RHG1 in agar plates as described above. To determine the RHG1 population on the shoots and roots, 10 shoots or roots were removed from the plates, pooled, and weighed at 10 DAIG, whereafter the samples were transferred to a sterile mortar and ground in 1 ml PBS solution, followed by successive 10-fold PSB dilutions from 10^{-1} to 10^{-8}. One hundred microliter of the diluted extract (10^{-6}, 10^{-7}, and 10^{-8} dilutions) was plated on a R2A medium plate. Three plates were plated for each dilution. The CFU/mg FW was determined after 3 days of incubation at 28°C. Three independent biological replicates were done.

Leaf cellular analysis

Four-day-old *Arabidopsis* seedlings were inoculated with RHG1. At 14 DPI, the total leaf blade area of cleared leaves was measured for both the first and second leaf of 15 plants per treatment under a dark-field binocular microscope. For three representative plants per treatment, the abaxial epidermal cells in the middle of the leaves were drawn with a microscope equipped with differential interference contrast optics (DM LB; Leica) and a drawing tube. Photographs of leaves and scanned cell drawings were used to measure leaf and cell area as described previously (Andriankaja et al. 2012).

GFP labeling of RHG1.

The mini-Tn*5*-based transposon delivery plasmid pUTgfp2x (Tombolini et al. 1997) was used for chromosomal insertion of the marker gene. The plasmid was introduced into RHG1 by triparental conjugation. The recipient strain RHG1 was grown overnight in PYE medium (0.2% [w/v] Bacto peptone, 0.1% [w/v] yeast extract, 1 mM $MgSO_4$, and 0.5 mM $CaCl_2$) and back diluted 1:15 into fresh medium, followed by a 5-hour incubation at 28°C. In parallel, the donor *Escherichia coli* strain pUTgfp2x and the helper *E. coli* strain pRK2013 were grown overnight in lysogeny broth medium and back diluted 1:100 into fresh medium, followed by a 5-hour incubation at 37°C. The resulting cultures were combined in a recipient:donor:helper ratio of 8:1:1, collected by centrifugation for 1 min at 5000*g*, and then grown on PYE agar plates without antibiotics to allow overnight conjugation. Transconjugants were selected on PYE agar supplemented with 50 µg/ml kanamycin to select for the RHG1 strain with

genomic integration of the marker gene and 20 µg/ml nalidixic acid to counterselect against the *E. coli* strains. Colonies with a green fluorescent phenotype were selected and further confirmed by PCR amplification of the *GFP* gene and by sequencing of the 16S gene.

Confocal microscopic analysis of colonization.

Arabidopsis seeds were inoculated with the GFP-tagged strain RHG1::GFP as described above. Fourteen-day-old plants were examined for colonization by means of live tissue or cleared tissue imaging. For live tissue imaging, plant samples were gently washed with half-strength MS medium, then mounted on microscope slides, and processed with an Olympus FluoView 1000 confocal microscope. For cleared tissue imaging, plants were fixed and cleared according the ClearSee protocol described previously (Kurihara et al. 2015). Briefly, plants were fixed with 4% paraformaldehyde in PBS solution for 1 h with vacuum treatment, whereafter they were rinsed twice with PBS solution. Subsequently, fixed samples were cleared in ClearSee solution (10% [w/v] xylitol, 15% [w/v] sodium deoxycholate, and 25% [w/v] urea in water) for 2 weeks at room temperature. Cleared samples were analyzed with a Zeiss LSM5 710 confocal microscope.

Genome sequencing, assembly, and annotation.

The *C.* sp. RHG1 genome was sequenced with an Illumina HiSeq 4000 platform (PE150 reads) at the Oxford Genomics Center. The quality of the reads was evaluated by means of the FastQC v0.11.8 software (Schmieder and Edwards, 2011). The assembly of the genome was achieved through the Shovill

pipeline that mainly applies SPAdes v3.12.0 (Bankevich et al. 2012). In addition, the Timmomatic v0.38 option in the Shovill pipeline was included into the command line to implement the trimming of the reads. The quality of the assembly was assessed with the software Quast v4.6.3 (Gurevich et al. 2013) and contigs smaller than 1000 bp were removed. The genome annotation was accomplished with the Rapid Annotation using Subsystem Technology (RAST) (Overbeek et al. 2014) and Prokka software (Seemann, 2014). BLAST v2.6.0 (Camacho et al. 2009) was used to verify the absence of the genes involved in plant growth promotion that were not present in the genome annotation of RHG1. The *C.* sp. RHG1 genome sequence data were deposited in the GenBank (https://www.ncbi.nlm.nih.gov/genbank/) under genome accession number SMZP00000000.

Phylogenomic analysis.

For the phylogenomic analysis of *C.* sp. RHG1, the genomes of 38 strains, previously classified within the genus *Caulobacter*, and three strains from the genus *Brevundimonas*, used as outgroup, were downloaded from the National Center for Biotechnology Information (NCBI) database (https://www.ncbi.nlm.nih.gov/). Initially, all the available genomes of the *Caulobacter* strains in the NCBI database were included into the analysis, but those that lacked several essential core genes were removed to avoid possible bias created by the presence of incomplete genomes. The bcgTree pipeline (Ankenbrand and Keller, 2016) was used to compare 107 essential bacterial core genes of the 43 strains. The comparison was done by performing 1000 bootstraps. Additionally, this pipeline generated a phylogenomic tree with RaxML

that was visualized with interactive Tree Of Life (iTOL) v4.2.3 (Letunic and Bork, 2016). Moreover, all strains were compared with the OrthoANIu (Yoon et al. 2017) method for their similarity determination.

Phylogenetic analysis.

Because not all the genome sequences were available for all 11 valid *Caulobacter* species, a maximum likelihood tree was constructed based on the available sequences of the 16S rRNA genes with the MEGA v10.0.5 software (Kumar et al. 2008).

***nirK* gene deletion strain construction.**

The *nirK* gene deletion was achieved through a recombination-based method with the allelic exchange vector pNPTS138 that contains the kanamycin resistance cassette and the sucrose-sensitive counterselection marker *sac*B (Ried and Collmer, 1987). To this end, a fused PCR product containing the 500-bp upstream region (amplified with the primers nirk_upstream_forward: aactgcagctcttccatgcaggcgatcg and nirk_upstream_reverse: gttgtagacaagattgatatctagatacacgttcctatccccgggcgcc) and the 500-bp downstream region (amplified with the primers nirk_downstream_forward: gtgtatctagatatcaatcttgtctacaacccctcgaaaccccggggcgg and nirk_downstream_reverse: ccggaattcgctcgttctgccgccaggccgag) of the *nirK* gene was cloned into the pNPTS138 vector. The resulting plasmid was introduced into RHG1 by conjugation through the *E. coli* strain S17-1 with kanamycin to select for the presence of the integrated plasmid DNA and with nalidixic acid to counterselect against *E. coli*. Colonies were further confirmed by PCR for plasmid

DNA integration and then grown in PYE medium overnight under nonselective conditions to allow a second recombination. Hereafter, cells were selected on PYE medium supplemented with 5% (w/v) sucrose and further tested for loss of kanamycin resistance. Sucrose-resistant and kanamycin-sensitive clones were further confirmed by PCR for the deletion of the *nirK* gene.

Western blot analysis of BES1 dephosphorylation.

Four-day-old wild-type *Arabidopsis* seedlings were mock-treated or inoculated with RHG1. Shoot and root samples separated from seedlings at 4 DPI were homogenized in liquid nitrogen. Total proteins were extracted with a buffer containing 20 mM Tris·HCl (pH 7.5), 150 mM NaCl, 1% (w/v) SDS, 100 mM DTT, and EDTA-free Protease Inhibitor Cocktail (Roche). For protein detection, the antibodies polyclonal α-BES1 (Yin et al. 2002), 1/4,000 dilution, and monoclonal α-Tubulin (Sigma-Aldrich), 1/10,000 dilution, were used. For the BES1 dephosphorylation assay, the ratio of the dephosphorylated BES1 to the total BES1 proteins was quantified based on the signal intensity. The loading was adjusted to an equal level based on the amount of tubulin. The signal intensity was determined with the Image Lab software.

GUS histochemical staining.

Four-day-old seedlings of the *DR5:GUS*, *pARR5:GUS,* and *pEBS:GUS* reporter lines were mock-treated or inoculated with *C.* sp. RHG1, and subjected to GUS histochemical staining at 4 DPI. Plants were incubated in GUS staining solution (100 mM Tris [pH 7], 50 mM NaCl, 1 mM $K_3[Fe(CN)_6]$, 2 mM 5-bromo-4-chloro-3-indolyl β-D-glucuronide cyclohexylammonium salt) overnight at 37°C,

followed by decoloring in 70% (v/v) ethanol. Plant shoot or root samples were examined under a stereomicroscope (Leica MZ16) or a differential interference contrast microscope (Olympus BX51), respectively.

Fluorescence microscopy.

For detection of the GFP signal in the *DR5:GFP* reporter line, 4-day-old seedlings were mock-treated or inoculated with *C.* sp. RHG1, followed by microscopic analysis at 4 DPI. Seedlings were stained with 10 µg/mL propidium iodide (PI) for 1 min and observed under an Olympus FluoView 1000 confocal microscope. The excitation wavelength was 488 nm for GFP and 559 nm for PI. Emission was detected at 500 to 530 nm for GFP and 580 to 619 nm for PI.

ACKNOWLEDGMENTS

We would like to thank Dr. Birgit Mitter and Dr. Stéphane Compant (Austrian Institute of Technology, Vienna, Austria) and Dr. Patrick H. Viollier (University of Geneva, Switzerland) for kindly providing the plasmid pUTgfp2x and pNPTS138, respectively, Alexandra Baekelandt for cellular analysis, and Martine De Cock for help in preparing the manuscript. This work was supported by a grant from the Research Foundation–Flanders (project no. G015118N) to A.W. and S.G.

LITERATURE CITED

Agler, M. T., Ruhe, J., Kroll, S., Morhenn, C., Kim, S.-T., Weigel, D., and Kemen, E. M. 2016. Microbial hub taxa link host and abiotic factors to plant microbiome variation. PLoS Biol. 14:e1002352.

Andriankaja, M., Dhondt, S., De Bodt, S., Vanhaeren, H., Coppens, F., De Milde, L., Mühlenbock, P., Skirycz, A., Gonzalez, N., Beemster, G. T. S., Inzé, D. 2012. Exit from proliferation during leaf development in *Arabidopsis thaliana*: a not-so-gradual process. Dev. Cell 22:64-78.

Ankenbrand, M. J., and Keller, A. 2016. bcgTree: automatized phylogenetic tree building from bacterial core genomes. Genome 59:783-791.

Bai, Y., Müller, D. B., Srinivas, G., Garrido-Oter, R., Potthoff, E., Rott, M., Dombrowski, N., Münch, P. C., Spaepen, S., Remus-Emsermann, M., Hüttel, B., McHardy, A. C., Vorholt, J. A., and Schulze-Lefert, P. 2015. Functional overlap of the *Arabidopsis* leaf and root microbiota. Nature 528:364-369.

Bankevich, A., Nurk, S., Antipov, D., Gurevich, A. A., Dvorkin, M., Kulikov, A. S., Lesin, V. M., Nikolenko, S. I., Pham, S., Prjibelski, A. D., Pyshkin, A. V., Sorotkin, A. V., Vyahhi, N., Tesler, G., Alekseyev, M. A., and Pevzner, P. A. 2012. SPAdes: a new genome assembly algorithm and its applications to single-cell sequencing. J. Comput. Biol. 19:455-477.

Benková, E., Michniewicz, M., Sauer, M., Teichmann, T., Seifertová, D., Jürgens, G., and Friml, J. 2003. Local, efflux-dependent auxin gradients as a common module for plant organ formation. Cell 115:591-602.

Berendsen, R. L., van Verk, M. C., Stringlis, I. A., Zamioudis, C., Tommassen, J., Pieterse, C. M. J., and Bakker, P. A. H. M. 2015. Unearthing the genomes of plant-beneficial *Pseudomonas* model strains WCS358, WCS374 and WCS417. BMC Genomics 16:539.

Berendsen, R. L., Vismans, G., Yu, K., Song, Y., de Jonge, R., Burgman, W. P., Burmølle, M., Herschend, J., Bakker, P. A. H. M., and Pieterse, C. M. J.

2018. Disease-induced assemblage of a plant-beneficial bacterial consortium. ISME J. 12:1496-1507.

Bhattacharyya, D., Garladinne, M., and Lee, Y. H. 2015. Volatile indole produced by rhizobacterium *Proteus vulgaris* JBLS202 stimulates growth of *Arabidopsis thaliana* through auxin, cytokinin, and brassinosteroid pathways. J. Plant Growth Regul. 34:158-168.

Creus, C. M., Graziano, M., Casanovas, E. M., Pereyra, M. A., Simontacchi, M., Puntarulo, S., Barassi, C. A., and Lamattina, L. 2005. Nitric oxide is involved in the *Azospirillum brasilense*-induced lateral root formation in tomato. Planta 221:297-303.

Camacho, C., Coulouris, G., Avagyan, V., Ma, N., Papadopoulos, J., Bealer, K., and Madden, T. L. 2009. BLAST+: architecture and applications. BMC Bioinformatics 10:421.

D'Agostino, I. B., Deruère, J., and Kieber, J. J. 2000. Characterization of the response of the Arabidopsis response regulator gene family to cytokinin. Plant Physiol. 124:1706-1717.

Dharmasiri, N., Dharmasiri, S., Weijers, D., Lechner, E., Yamada, M., Hobbie, L., Ehrismann, J. S., Jürgens, G., and Estelle, M. 2005. Plant development is regulated by a family of auxin receptor F box proteins. Dev. Cell 9:109-119.

Edulamudi, P., Masilamani, A. J. A., Divi, V. R. S. G., and Konada, V. M. 2011. Novel root nodule bacteria belonging to the genus *Caulobacter*. Lett. Appl. Microbiol. 53:587-591.

Fitzpatrick, C. R., Copeland, J., Wang, P. W., Guttman, D. S., Kotanen, P. M., and Johnson, M. T. J. 2018. Assembly and ecological function of the root

microbiome across angiosperm plant species. Proc. Natl. Acad. Sci. USA 115:E1157-E1165.

Glick, B. R. 2014. Bacteria with ACC deaminase can promote plant growth and help to feed the world. Microbiol. Res. 169:30-39.

Gouda, S., Kerry, R. G., Das, G., Paramithiotis, S., Shin, H.-S., and Patra, J. K. 2018. Revitalization of plant growth promoting rhizobacteria for sustainable development in agriculture. Microbiol. Res. 206:131-140.

Gurevich, A., Saveliev, V., Vyahhi, N., and Tesler, G. 2013. QUAST: quality assessment tool for genome assemblies. Bioinformatics 29:1072-1075.

Hontzeas, N., Zoidakis, J., Glick, B. R., and Abu-Omar, M. M. 2004. Expression and characterization of 1-aminocyclopropane-1-carboxylate deaminase from the rhizobacterium *Pseudomonas putida* UW4: a key enzyme in bacterial plant growth promotion. Biochim. Biophys. Acta 1703:11-19.

Jaillais, Y., Belkhadir, Y., Balsemão-Pires, E., Dangl, J. L., and Chory, J. 2011. Extracellular leucine-rich repeats as a platform for receptor/coreceptor complex formation. Proc. Natl. Acad. Sci. USA 108:8503-8507.

Jensen, P. J., Hangarter, R. P., and Estelle, M. 1998. Auxin transport is required for hypocotyl elongation in light-grown but not dark-grown Arabidopsis. Plant Physiol. 116:455-462.

Kalve, S., De Vos, D., and Beemster, G. T. S. 2014. Leaf development: a cellular perspective. Front. Plant Sci. 5:362.

Kanchiswamy, C. N., Malnoy, M., and Maffei, M. E. 2015. Bioprospecting bacterial and fungal volatiles for sustainable agriculture. Trends Plant Sci. 20:206-211.

Kumar, S., Nei, M., Dudley, J., and Tamura, K. 2008. MEGA: a biologist-centric software for evolutionary analysis of DNA and protein sequences. Brief. Bioinformatics 9:299-306.

Kurihara, D., Mizuta, Y., Sato, Y., and Higashiyama, T. 2015. ClearSee: a rapid optical clearing reagent for whole-plant fluorescence imaging Development 142:4168-4179.

Kwak, M.-J., Kong, H. G., Choi, K., Kwon, S.-K., Song, J. Y., Lee, J., Lee, P. A., Choi, S. Y., Seo, M., Lee, H. J., Jung, E. J., Park, H., Roy, N., Kim, H. Lee, M. M., Rubin, E. M., Lee, S.-W., and Kim, J. F. 2018. Rhizosphere microbiome structure alters to enable wilt resistance in tomato. Nat. Biotechnol. 36:1100-1109.

Lemanceau, P., Blouin, M., Muller, D., and Moënne-Loccoz, Y. 2017. Let the core microbiota be functional. Trends Plant Sci. 22:583-595.

Letunic, I., and Bork, P. 2016. Interactive tree of life (iTOL) v3: an online tool for the display and annotation of phylogenetic and other trees. Nucleic Acids Res. 44:W242-W245.

Liu, F., Xing, S., Ma, H., Du, Z., and Ma, B. 2013. Cytokinin-producing, plant growth-promoting rhizobacteria that confer resistance to drought stress in *Platycladus orientalis* container seedlings. Appl. Microbiol. Biotechnol. 97:9155-9164.

Mitter, B., Petric, A., Shin, M. W., Chain, P. S. G., Hauberg-Lotte, L., Reinhold-Hurek, B., Nowak, J., and Sessitsch, A. 2013. Comparative genome analysis of *Burkholderia phytofirmans* PsJN reveals a wide spectrum of endophytic lifestyles based on interaction strategies with host plants. Front. Plant Sci. 4:120.

Moya, G., Yan, Z.-F., Won, K., Yang, J.-E., Wang, Q.-J., Kook, M., and Yi, T.-H. 2017. *Caulobacter hibisci* sp. nov., isolated from rhizosphere of *Hibiscus syriacus* L. (Mugunghwa flower). Int. J. Syst. Evol. Microbiol. 67:3167-3173.

Nishimura, C., Ohashi, Y., Sato, S., Kato, T., Tabata, S., and Ueguchi, C. 2004. Histidine kinase homologs that act as cytokinin receptors possess overlapping functions in the regulation of shoot and root growth in Arabidopsis. Plant Cell 16:1365-1377.

Overbeek, R., Olson, R., Pusch, G. D., Olsen, G. J., Davis, J. J., Disz, T., Edwards, R. A., Gerdes, S., Parrello, B., Shukla, M., Vonstein, V., Wattam, A. R., Xia, F., and Stevens, R. 2014. The SEED and the Rapid Annotation of microbial genomes using Subsystems Technology (RAST). Nucleic Acids Res. 42:D206-D214.

Pallai, R., Hynes, R. K., Verma, B., and Nelson, L. M. 2012. Phytohormone production and colonization of canola (*Brassica napus* L.) roots by *Pseudomonas fluorescens* 6-8 under gnotobiotic conditions. Can. J. Microbiol. 58:170-178.

Pieterse, C. M. J., van Wees, S. C. M., van Pelt, J. A., Knoester, M., Laan, R., Gerrits, H., Weisbeek, P. J., and van Loon, L. C. 1998. A novel signaling pathway controlling induced systemic resistance in Arabidopsis. Plant Cell 10:1571-1580.

Pieterse, C. M. J., Zamioudis, C., Berendsen, R. L., Weller, D. M., Van Wees, S. C. M., and Bakker, P. A. H. M. 2014. Induced systemic resistance by beneficial microbes. Annu. Rev. Phytopathol. 52:347-375.

Pothier, J. F., Prigent-Combaret, C., Haurat, J., Moënne-Loccoz, Y., and Wisniewski-Dyé, F. 2008. Duplication of plasmid-borne nitrite reductase gene *nirK* in the wheat-associated plant growth--promoting rhizobacterium *Azospirillum brasilense* Sp245. Mol. Plant-Microbe Interact. 21:831-842.

Reasoner, D. J., and Geldreich, E. E. 1985. A new medium for the enumeration and subculture of bacteria from potable water. Appl. Environ. Microbiol. 49:1-7.

Richardson, A. E., Barea, J.-M., McNeill, A. M., and Prigent-Combaret, C. 2009. Acquisition of phosphorus and nitrogen in the rhizosphere and plant growth promotion by microorganisms. Plant Soil 321:305-339.

Ried, J. L., and Collmer, A. 1987. An *nptI-sacB-sacR* cartridge for constructing directed, unmarked mutations in Gram-negative bacteria by marker exchange-eviction mutagenesis. Gene 57:239-246.

Saini, S., Sharma, I., and Pati, P. K. 2015. Versatile roles of brassinosteroid in plants in the context of its homoeostasis, signaling and crosstalks. Front. Plant Sci. 6:950.

Sami, F., Faizan, M., Faraz, A., Siddiqui, H., Yusuf, M., and Hayat, S. 2018. Nitric oxide-mediated integrative alterations in plant metabolism to confer abiotic stress tolerance, NO crosstalk with phytohormones and NO-mediated post translational modifications in modulating diverse plant stress. Nitric Oxide 73:22-38.

Schaller, G. E., Street, I. H., and Kieber, J. J. 2014. Cytokinin and the cell cycle. Curr. Opin. Plant Biol. 21:7-15.

Schmieder, R., and Edwards, R. 2011. Quality control and preprocessing of metagenomic datasets. Bioinformatics 27:863-864.

Seemann, T. 2014. Prokka: rapid prokaryotic genome annotation. Bioinformatics 30:2068-2069.

Sévin, D. C., Fuhrer, T., Zamboni, N., and Sauer, U. 2017. Nontargeted *in vitro* metabolomics for high-throughput identification of novel enzymes in *Escherichia coli*. Nat. Methods 14:187-194.

Spaepen, S., Bossuyt, S., Engelen, K., Marchal, K., and Vanderleyden, J. 2014. Phenotypical and molecular responses of *Arabidopsis thaliana* roots as a result of inoculation with the auxin-producing bacterium *Azospirillum brasilense*. New Phytol. 201:850-861.

Stepanova, A. N., Yun, J., Likhacheva, A. V., and Alonso, J. M. 2007. Multilevel interactions between ethylene and auxin in *Arabidopsis* roots. Plant Cell 19:2169-2185.

Stringlis, I. A., Proietti, S., Hickman, R., Van Verk, M. C., Zamioudis, C., and Pieterse, C. M. J. 2018. Root transcriptional dynamics induced by beneficial rhizobacteria and microbial immune elicitors reveal signatures of adaptation to mutualists. Plant J. 93:166-180.

Sun, L.-N., Yang, E.-D., Hou, X.-T., Wei, J.-C., Yuan, Z.-X., and Wang, W.-Y. 2017. *Caulobacter rhizosphaerae* sp. nov., a stalked bacterium isolated from rhizosphere soil. Int. J. Syst. Evol. Microbiol. 67:1771-1776.

Szekeres, M., Németh, K., Koncz-Kálmán, Z., Mathur, J., Kauschmann, A., Altmann, T., Rédei, G. P., Nagy, F., Schell, J., and Koncz, C. 1996. Brassinosteroids rescue the deficiency of CYP90, a cytochrome P450,

controlling cell elongation and de-etiolation in Arabidopsis. Cell 85:171-182.

Tahir, H. A. S., Gu, Q., Wu, H., Raza, W., Hanif, A., Wu, L., Colman, M. V., and Gao, X. 2017. Plant growth promotion by volatile organic compounds produced by *Bacillus subtilis* SYST2. Front. Microbiol. 8:171.

Toju, H., Peay, K. G., Yamamichi, M., Narisawa, K., Hiruma, K., Naito, K., Fukuda, S., Ushio, M., Nakaoka, S., Onoda, Y., Yoshida, K., Schlaeppi, K., Bai, Y., Sugiura, R., Ichihashi, Y., Minamisawa, K., and Kiers, E. T. 2018. Core microbiomes for sustainable agroecosystems. Nat. Plants 4:247-257.

Tombolini, R., Unge, A., Davey, M. E., de Bruijn, F. J., and Jansson, J. K. 1997. Flow cytometric and microscopic analysis of GFP-tagged *Pseudomonas fluorescens* bacteria. FEMS Microbiol. Ecol. 22:17-28.

Tsukanova, K. A., Chebotar, V. K., Meyer, J. J. M., and Bibikova, T. N. 2017. Effect of plant growth-promoting rhizobacteria on plant hormone homeostasis. S. Afr. J. Bot. 113:91-102.

Ulmasov, T., Murfett, J., Hagen, G., and Guilfoyle, T. J. 1997. Aux/IAA proteins repress expression of reporter genes containing natural and highly active synthetic auxin response elements. Plant Cell 9:1963-1971.

Vacheron, J., Desbrosses, G., Bouffaud, M.-L., Touraine, B., Moënne-Loccoz, Y., Muller, D., Legendre, L., Wisniewski-Dyé, F., and Prigent-Combaret, C. 2013. Plant growth-promoting rhizobacteria and root system functioning. Front. Plant Sci. 4:356.

Vacheron, J., Desbrosses, G., Renoud, S., Padilla, R., Walker, V., Muller, D., and Prigent-Combaret, C. 2018. Differential contribution of plant-

beneficial functions from *Pseudomonas kilonensis* F113 to root system architecture alterations in *Arabidopsis thaliana* and *Zea mays*. Mol. Plant-Microbe Interact. 31:212-223.

Van Deynze, A., Zamora, P., Delaux, P.-M., Heitmann, C., Jayaraman, D., Rajasekar, S., Graham, D., Maeda, J., Gibson, D., Schwartz, K. D., Berry, A. M., Bhatnagar, S., Jospin, G., Darling, A., Jeannotte, R., Lopez, J., Weimer, B. C., Eisen, J. A., Shapiro, H.-Y., Ané, J.-M., and Bennett, A. B. 2018. Nitrogen fixation in a landrace of maize is supported by a mucilage-associated diazotrophic microbiota. PLoS Biol. 16:e2006352.

Walters, W. A., Jin, Z., Youngblut, N., Wallace, J. G., Sutter, J., Zhang, W., González-Peña, A., Peiffer, J., Koren, O., Shi, Q., Knight, R., del Rio, T. G., Tringe, S. G., Buckler, E. S., Dangl, J. L., and Ley, R. E. 2018. Large-scale replicated field study of maize rhizosphere identifies heritable microbes. Proc. Natl. Acad. Sci. USA 115:7368-7373.

Wang, J., Zhang, Y., Li, Y., Wang, X., Nan, W., Hu, Y., Zhang, H., Zhao, C., Wang, F., Li, P., Shi, H., and Bi, Y. 2015. Endophytic microbes *Bacillus* sp. LZR216-regulated root development is dependent on polar auxin transport in *Arabidopsis* seedlings. Plant Cell Rep. 34:1075-1087.

Wang, Y., Liu, C., Li, K., Sun, F., Hu, H., Li, X., Zhao, Y., Han, C., Zhang, W., Duan, Y., Liu, M., and Li, X. 2007. *Arabidopsis EIN2* modulates stress response through abscisic acid response pathway. Plant Mol Biol. 64:633-644.

Woldemeskel, S. A., and Goley, E. D. 2017. Shapeshifting to survive: shape determination and regulation in *Caulobacter crescentus*. Trends Microbiol. 25:673-687.

Yin, Y., Wang, Z.-Y., Mora-Garcia, S., Li, J., Yoshida, S., Asami, T., and Chory, J. 2002. BES1 accumulates in the nucleus in response to brassinosteroids to regulate gene expression and promote stem elongation. Cell 109:181-191.

Yoon, S.-H., Ha, S.-m., Lim, J., Kwon, S., and Chun, J. 2017. A large-scale evaluation of algorithms to calculate average nucleotide identity. Antonie Leeuwenhoek 110:1281-1286.

Zamioudis, C., Mastranesti, P., Dhonukshe, P., Blilou, I., and Pieterse, C. M. J. 2013. Unraveling root developmental programs initiated by beneficial *Pseudomonas* spp. bacteria. Plant Physiol. 162:304-318.

Zhao, Y., Christensen, S. K., Fankhauser, X., Cashman, J. R., Cohen, J. D., Weigel, D., and Chory, J. 2001. A role for flavin monooxygenase-like enzymes in auxin biosynthesis. Science 291:306-309.

Zumft, W. G. 1997. Cell biology and molecular basis of denitrification. Microbiol. Mol. Biol. Rev. 61:533-616.

Legends to figures

Fig. 1. Plant growth promotion effect of RHG1 in *Arabidopsis.* Seeds were mock-treated or inoculated with RHG1 in an *in vitro* system and the different growth parameters were determined at 14 or 18 DAIG. **A**, Representative photographs of mock-treated or RHG1-inoculated *Arabidopsis* seedlings at 18 DAIG. Bar = 1 cm. **B to G**, Effects of RHG1 on different parameters of *Arabidopsis* plant growth. Fresh weight (**B**), third leaf area (**C**), and leaf number (**D**) were determined at 18 DAIG, and lateral root number (**E**), lateral root density (**F**), and total root length (**G**) at 14 DAIG. The plot graphs are based on three biological replicates ($n \geq 12$ for each treatment). Asterisks indicate significant differences between mock and inoculated plants (** $P < 0.01$, Student's *t*-test). M, mock-treated; RHG1, RHG1-inoculated.

Fig. 2. Increased cell number and reduced cell area in leaves by RHG1 inoculation. **A** and **B**, Representative pictures of abaxial epidermal cells in leaves of mock-treated (**A**) and RHG1-inoculated (**B**) plants. Bar = 100 µm. **C** and **D**, Average number of pavement cells, guard cells, and total cells per leaf (**C**), and average pavement cell area (**D**). Mean ± SE. The graphs are based on three biological replicates with six leaves for each treatment per replicate. Asterisks indicate significant differences between mock and inoculated plants (** $P < 0.01$; * $P < 0.05$. Student's *t*-test). M, mock-treated; RHG1, RHG1-inoculated.

Fig. 3. RHG1::GFP colonization of *Arabidopsis*. Confocal microscopic images of *Arabidopsis* colonized by strain RHG1::GFP. Seeds were inoculated with

RHG1::GFP. At 14 DAIG, plants were directly subjected to confocal microscopic imaging (**A** to **E**) or cleared in ClearSee buffer for 2 weeks followed by confocal microscopic imaging (**F** to **H**). **A** and **B**, RHG1::GFP colonization on the surface of the abaxial side (**A**) and adaxial side (**B**) of the leaf. **C** to **H**, RHG1::GFP colonization of the root at the root tip (**C** and **F**), mature zone (**D** and **G**), and lateral root emergence (**E** and **H**). Bar = 30 μm.

Fig. 4. Effects of RHG1 and RHG1 △*nirK* inoculation on different parameters of the *Arabidopsis* plant growth. Seeds were mock treated (M) or inoculated with the wild-type RHG1 strain (RHG1) or the RHG1 △*nirK* mutant strain (△*nirK*). **A** and **B,** Lateral root number and lateral root density determined at 14 DAIG, respectively. **C,** Fresh weights of shoots and roots determined at 18 DAIG. Data of three independent biological repeats were combined ($n \geq 15$). Asterisks indicate significant differences between different treatments (** $P < 0.01$; ns, $P > 0.05$. Student's *t*-test).

Fig. 5. Responses of the auxin-responsive marker lines and mutants/transgenic line to RHG1. **A**, Expression of *DR5:GUS* (left and middle) and *DR5:GFP* (right) in mock-treated (top) and RHG1-inoculated (bottom) plants, respectively. Four-day-old *Arabidopsis* seedlings were inoculated and subjected to GUS staining or confocal microscopic imaging at 4 DPI. Three independent replicates were done. Bars = 1 mm and 0.1 mm for shoot and root images, respectively. **B**, Effect of RHG1 on total plant fresh weight in Col-0, *yucca1D, 35S:iaaL*, and *tir1afb2/3. Arabidopsis* seeds were mock-treated or inoculated with RHG1. Fresh weight was determined at 18 DAIG from at least 15 plants per treatment. Results of three

independent replicates were combined and shown in the plot graph. The value on top of the two boxes of each genotype indicates the fold change in weight between mock-treated (M) and RHG1-inoculated (RHG1) plants. Asterisks indicate significant differences between mock and inoculated plants (** $P < 0.01$, Student's *t*-test).

Fig. 6. Response of cytokinin- and ethylene-responsive marker lines and mutants to RHG1. **A** and **C**, Expression of *pARR5:GUS* and *pEBS:GUS* in mock-treated and RHG1-inoculated plants, respectively. Plants were inoculated at 4 DAIG and subjected to GUS staining at 4 DPI. For *pARR5:GUS* (**A**), representative pictures of all six plants grown in one plate for mock treatment or RHG1 inoculation are shown, because of the variation in GUS staining between the plants. Three independent replicates were performed. Bars = 5 mm (**A**) and 1 mm (**C**) for shoot and 0.1 mm for root images. **B** and **D**, Effect of RHG1 on *Arabidopsis* shoot and root fresh weights, respectively, in Col-0, *ein2-5,* and *ahk234.* Seeds were mock-treated or inoculated with RHG1. Fresh weight was determined at 18 DAIG from at least 20 plants per treatment. Results of four independent replicates were combined and shown in the plot graphs. The value on top of the two boxes of each genotype indicates the fold change in weight between mock-treated (M) and RHG1-inoculated (RHG1) plants. Asterisks indicate significant differences between mock and inoculated plants (** $P < 0.01$, Student's *t*-test).

Fig. 7. Role of the brassinosteroid pathway in the plant-RHG1 interaction. **A**, Effect of RHG1 on plant fresh weight in Col-0, *cpd,* and *bri1.* Five-day-old seedlings were mock-treated (M) or inoculated with RHG1 (RHG1). Total fresh

plant weight was determined at 14 DPI. Four independent repeats were performed ($n \geq 15$). The result of one replicate is shown (see also Supplementary Fig. 7, for the other three independent replicates). The value on top of the two boxes of each genotype indicates the fold change in weight between mock-treated (M) and RHG1-inoculated (RHG1) plants. Asterisks indicate significant differences between mock and inoculated plants (** $P < 0.01$; ns, $P > 0.05$. Student's *t*-test). **B**, Western blot analysis of BES1 dephosphorylation. Proteins were extracted from mock-treated (M) or RHG1-inoculated (RHG1) shoots or roots of wild-type Col-0 plants at 4 DPI, followed by Western blot with the antibody against BES1. The protein inputs were equilibrated with the antibody against tubulin. The percentage of dephosphorylated BES1 relative to the total BES1 from three biological replicates is shown. ns, $P > 0.05$, Student's *t*-test.

Table 1. Presence of traits in the RHG1 genome related to plant growth promotion and endophytic lifestyle.

Category	Function	Gene no.	NODE	Start	End
Polymer-degrading enzymes	Polysaccharide lyase family	1	3	33609	34985
	Glycosyl hydrolases family	1	1	81572	82603
		1	1	121418	123883
		1	5	382168	384420
		1	9	47554	50001
ROS-detoxifying enzymes	Catalase	1	2	349951	352044
		1	5	68245	69693
		1	10	164194	165648
	Peroxidase	1	3	343660	344496
		1	5	71385	72365
		1	7	92478	92939
	Superoxide dismutase	1	3	657325	657942
		1	11	146429	146953
Motility and Chemotaxis	Flagellar motility	8	1	133513	139962
		3	1	444115	446245
		5	1	664047	665673
		11	2	72375	80644
		13	8	209728	225726
	Chemotaxis	6	2	130282	137690
		7	5	297807	304828
		14	5	390511	405982
Biofertilization	Phosphate solubilization	-	-	-	-
	Nitrogen fixation	-	-	-	-
Biocontrol	DAPG biosynthesis	-	-	-	-
	Cyanhidric acid biosynthesis	-	-	-	-
Denitrification	Copper-containing nitrite reductase	1	2	236063	237094
	Nitrite reductase [NAD(P)H] small and large subunit	2	2	114040	116852
	NO reductase	1	1	281420	283696
		1	2	230222	232495
	NO-responding transcriptional activator NnrR	1	2	234107	234802
Phytohormone modulation	ACC deaminase	-	-	-	-
	Indole-3-acetic acid biosynthesis	-	-	-	-
	Gibberellin biosynthesis	-	-	-	-

Cytokinin biosynthesis	-	-	-	-
Abscisic acid biosynthesis	-	-	-	-

-, no gene found for the category.

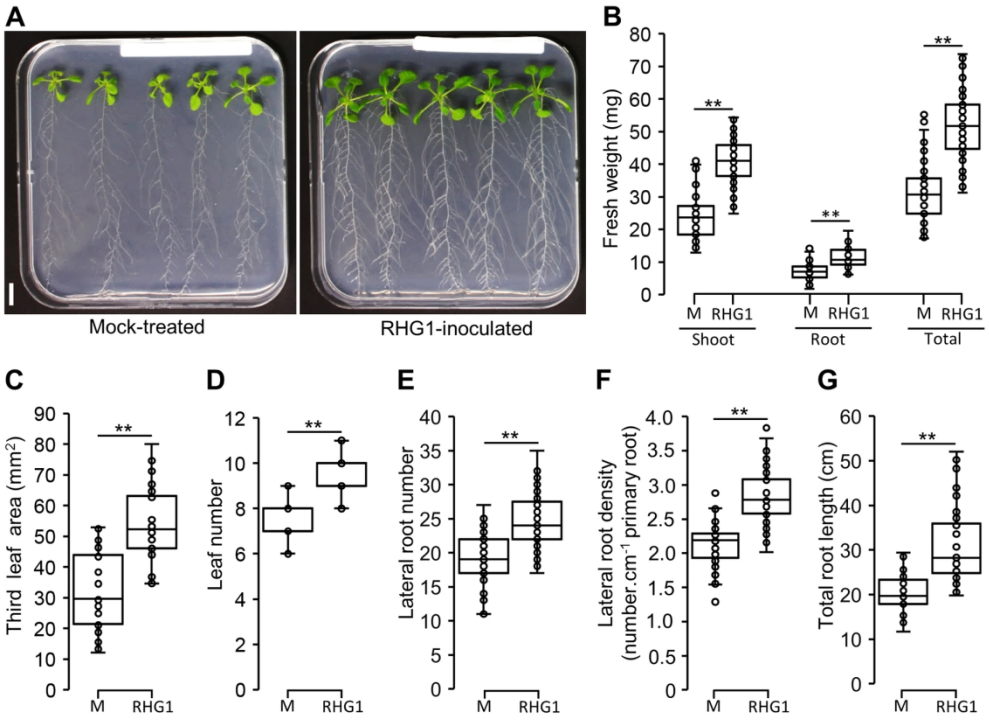

Fig. 1. Plant growth promotion effect of RHG1 in Arabidopsis. Seeds were mock-treated or inoculated with RHG1 in an in vitro system and the different growth parameters were determined at 14 or 18 DAIG. A, Representative photographs of mock-treated or RHG1-inoculated Arabidopsis seedlings at 18 DAIG. Bar = 1 cm. B to G, Effects of RHG1 on different parameters of Arabidopsis plant growth. Fresh weight (B), third leaf area (C), and leaf number (D) were determined at 18 DAIG, and lateral root number (E), lateral root density (F), and total root length (G) at 14 DAIG. The plot graphs are based on three biological replicates (n ≥ 12 for each treatment). Asterisks indicate significant differences between mock and inoculated plants (** P < 0.01, Student's t-test). M, mock-treated; RHG1, RHG1-inoculated.

161x115mm (300 x 300 DPI)

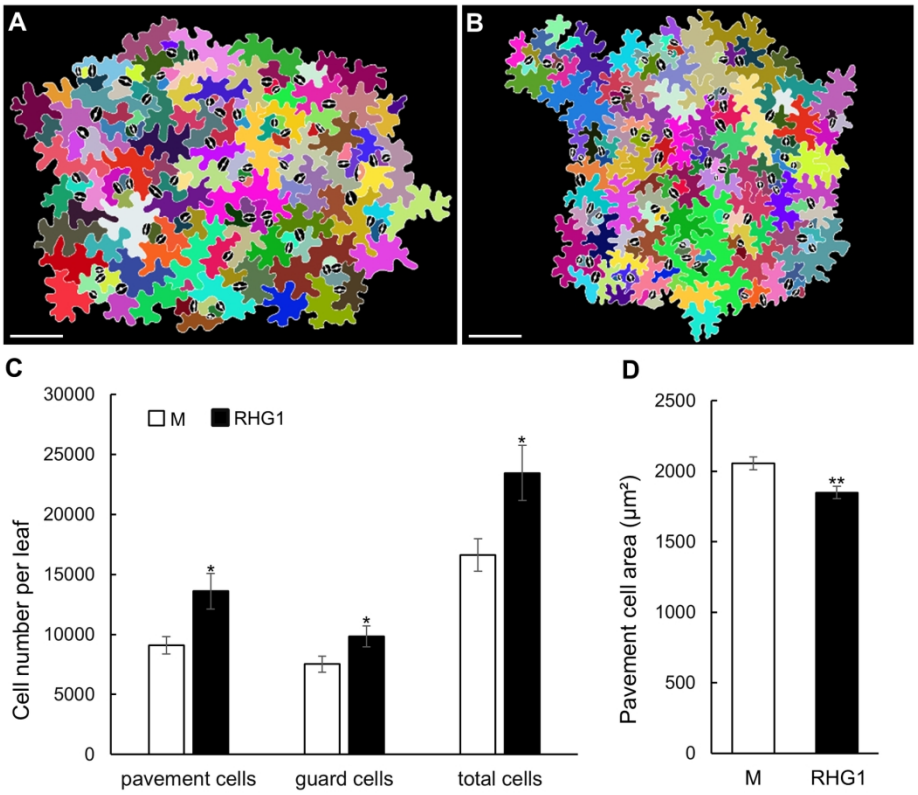

Fig. 2. Increased cell number and reduced cell area in leaves by RHG1 inoculation. A and B, Representative pictures of abaxial epidermal cells in leaves of mock-treated (A) and RHG1-inoculated (B) plants. Bar = 100 μm. C and D, Average number of pavement cells, guard cells, and total cells per leaf (C), and average pavement cell area (D). Mean ± SE. The graphs are based on three biological replicates with six leaves for each treatment per replicate. Asterisks indicate significant differences between mock and inoculated plants (** P < 0.01; * P < 0.05. Student's t-test). M, mock-treated; RHG1, RHG1-inoculated.

173x136mm (300 x 300 DPI)

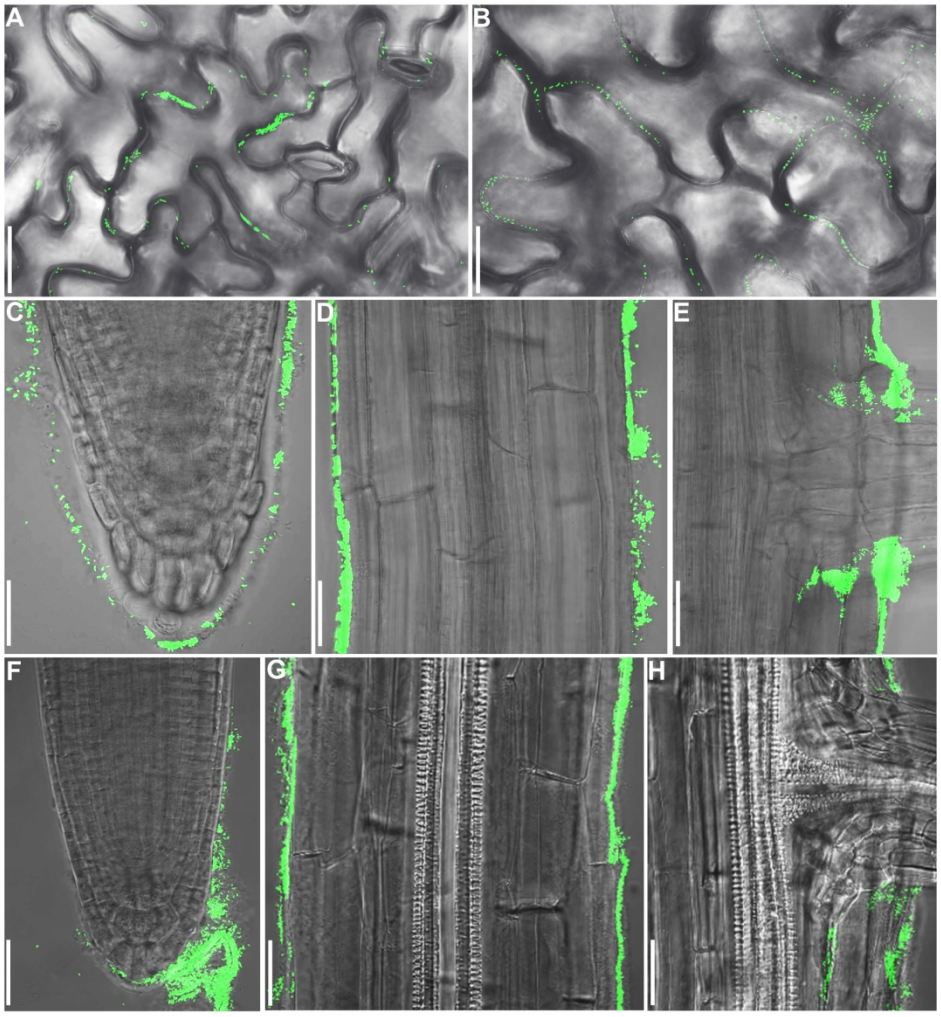

Fig. 3. RHG1::GFP colonization of Arabidopsis. Confocal microscopic images of Arabidopsis colonized by strain RHG1::GFP. Seeds were inoculated with RHG1::GFP. At 14 DAIG, plants were directly subjected to confocal microscopic imaging (A to E) or cleared in ClearSee buffer for 2 weeks followed by confocal microscopic imaging (F to H). A and B, RHG1::GFP colonization on the surface of the abaxial side (A) and adaxial side (B) of the leaf. C to H, RHG1::GFP colonization of the root at the root tip (C and F), mature zone (D and G), and lateral root emergence (E and H). Bar = 30 μm.

170x171mm (300 x 300 DPI)

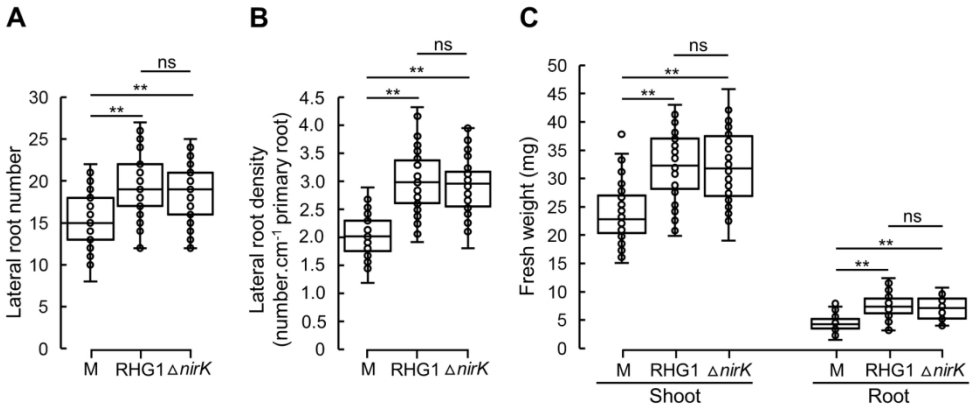

Fig. 4. Effects of RHG1 and RHG1 ΔnirK inoculation on different parameters of the Arabidopsis plant growth. Seeds were mock treated (M) or inoculated with the wild-type RHG1 strain (RHG1) or the RHG1 ΔnirK mutant strain (ΔnirK). A and B, Lateral root number and lateral root density determined at 14 DAIG, respectively. C, Fresh weights of shoots and roots determined at 18 DAIG. Data of three independent biological repeats were combined (n ≥ 15). Asterisks indicate significant differences between different treatments (** P < 0.01; ns, P > 0.05. Student's t-test).

161x65mm (300 x 300 DPI)

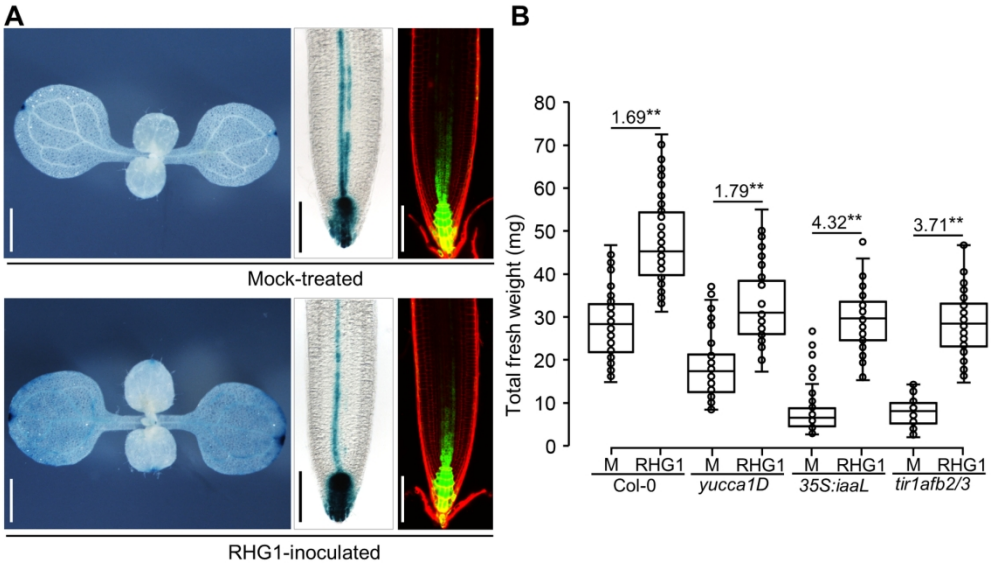

Fig. 5. Responses of the auxin-responsive marker lines and mutants/transgenic line to RHG1. A, Expression of DR5:GUS (left and middle) and DR5:GFP (right) in mock-treated (top) and RHG1-inoculated (bottom) plants, respectively. Four-day-old Arabidopsis seedlings were inoculated and subjected to GUS staining or confocal microscopic imaging at 4 DPI. Three independent replicates were done. Bars = 1 mm and 0.1 mm for shoot and root images, respectively. B, Effect of RHG1 on total plant fresh weight in Col-0, yucca1D, 35S:iaaL, and tir1afb2/3. Arabidopsis seeds were mock-treated or inoculated with RHG1. Fresh weight was determined at 18 DAIG from at least 15 plants per treatment. Results of three independent replicates were combined and shown in the plot graph. The value on top of the two boxes of each genotype indicates the fold change in weight between mock-treated (M) and RHG1-inoculated (RHG1) plants. Asterisks indicate significant differences between mock and inoculated plants (** $P < 0.01$, Student's t-test).

161x90mm (300 x 300 DPI)

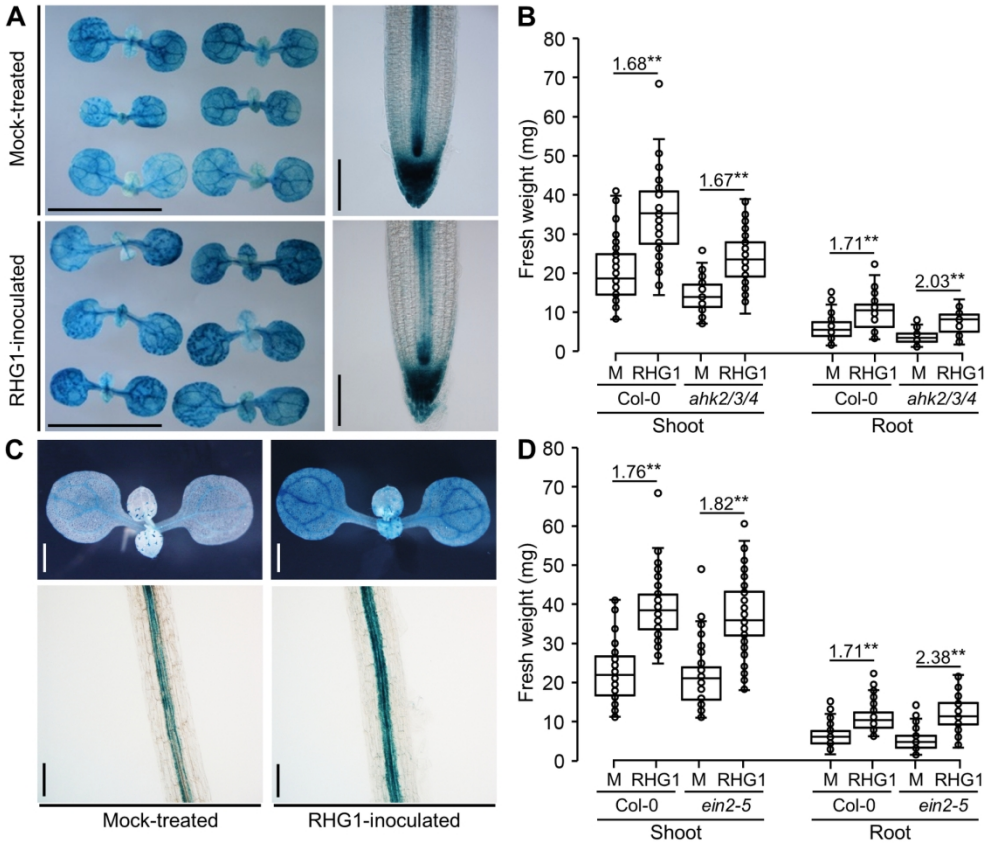

Fig. 6. Response of cytokinin- and ethylene-responsive marker lines and mutants to RHG1. A and C, Expression of pARR5:GUS and pEBS:GUS in mock-treated and RHG1-inoculated plants, respectively. Plants were inoculated at 4 DAIG and subjected to GUS staining at 4 DPI. For pARR5:GUS (A), representative pictures of all six plants grown in one plate for mock treatment or RHG1 inoculation are shown, because of the variation in GUS staining between the plants. Three independent replicates were performed. Bars = 5 mm (A) and 1 mm (C) for shoot and 0.1 mm for root images. B and D, Effect of RHG1 on Arabidopsis shoot and root fresh weights, respectively, in Col-0, ein2-5, and ahk234. Seeds were mock-treated or inoculated with RHG1. Fresh weight was determined at 18 DAIG from at least 20 plants per treatment. Results of four independent replicates were combined and shown in the plot graphs. The value on top of the two boxes of each genotype indicates the fold change in weight between mock-treated (M) and RHG1-inoculated (RHG1) plants. Asterisks indicate significant differences between mock and inoculated plants (** $P < 0.01$, Student's t-test).

161x136mm (300 x 300 DPI)

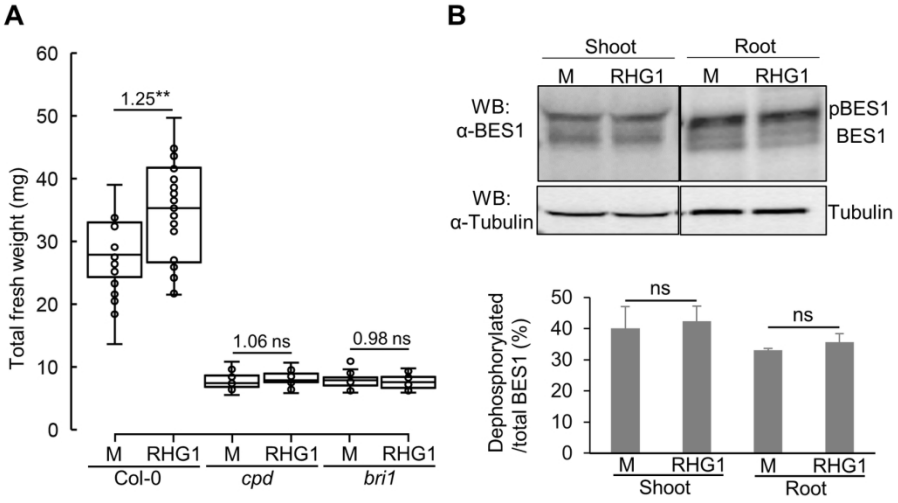

Fig. 7. Role of the brassinosteroid pathway in the plant-RHG1 interaction. A, Effect of RHG1 on plant fresh weight in Col-0, cpd, and bri1. Five-day-old seedlings were mock-treated (M) or inoculated with RHG1 (RHG1). Total fresh plant weight was determined at 14 DPI. Four independent repeats were performed (n ≥ 15). The result of one replicate is shown (see also Supplementary Fig. 7, for the other three independent replicates). The value on top of the two boxes of each genotype indicates the fold change in weight between mock-treated (M) and RHG1-inoculated (RHG1) plants. Asterisks indicate significant differences between mock and inoculated plants (** $P < 0.01$; ns, $P > 0.05$. Student's t-test). B, Western blot analysis of BES1 dephosphorylation. Proteins were extracted from mock-treated (M) or RHG1-inoculated (RHG1) shoots or roots of wild-type Col-0 plants at 4 DPI, followed by Western blot with the antibody against BES1. The protein inputs were equilibrated with the antibody against tubulin. The percentage of dephosphorylated BES1 relative to the total BES1 from three biological replicates is shown. ns, $P > 0.05$, Student's t-test.

161x80mm (300 x 300 DPI)

SUPPLEMENTARY FIGURES

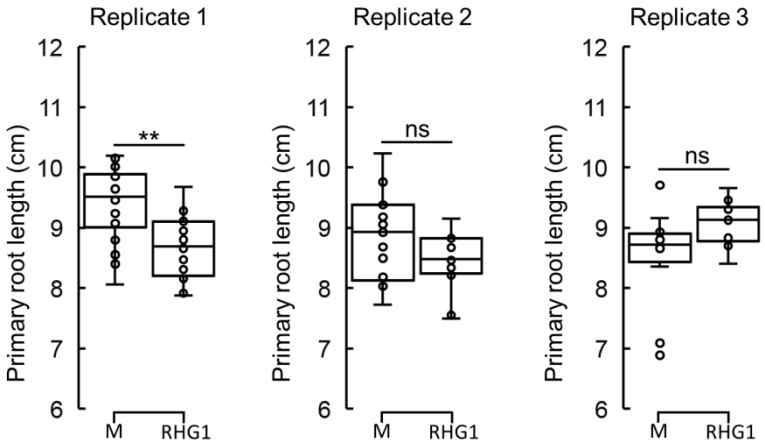

Supplementary Fig. 1. Variable effects of RHG1 on the primary root length of *Arabidopsis*. *Arabidopsis* seeds were mock-treated or inoculated with RHG1. Graphs show the primary root length of mock-treated (M) and RHG1-inoculated (RHG1) seedlings at 14 DAIG in three independent replicates ($n \geq 12$ for each treatment). Asterisks indicate significant differences between mock and inoculated plants (** $P < 0.01$; ns, $P > 0.05$. Student's *t*-test).

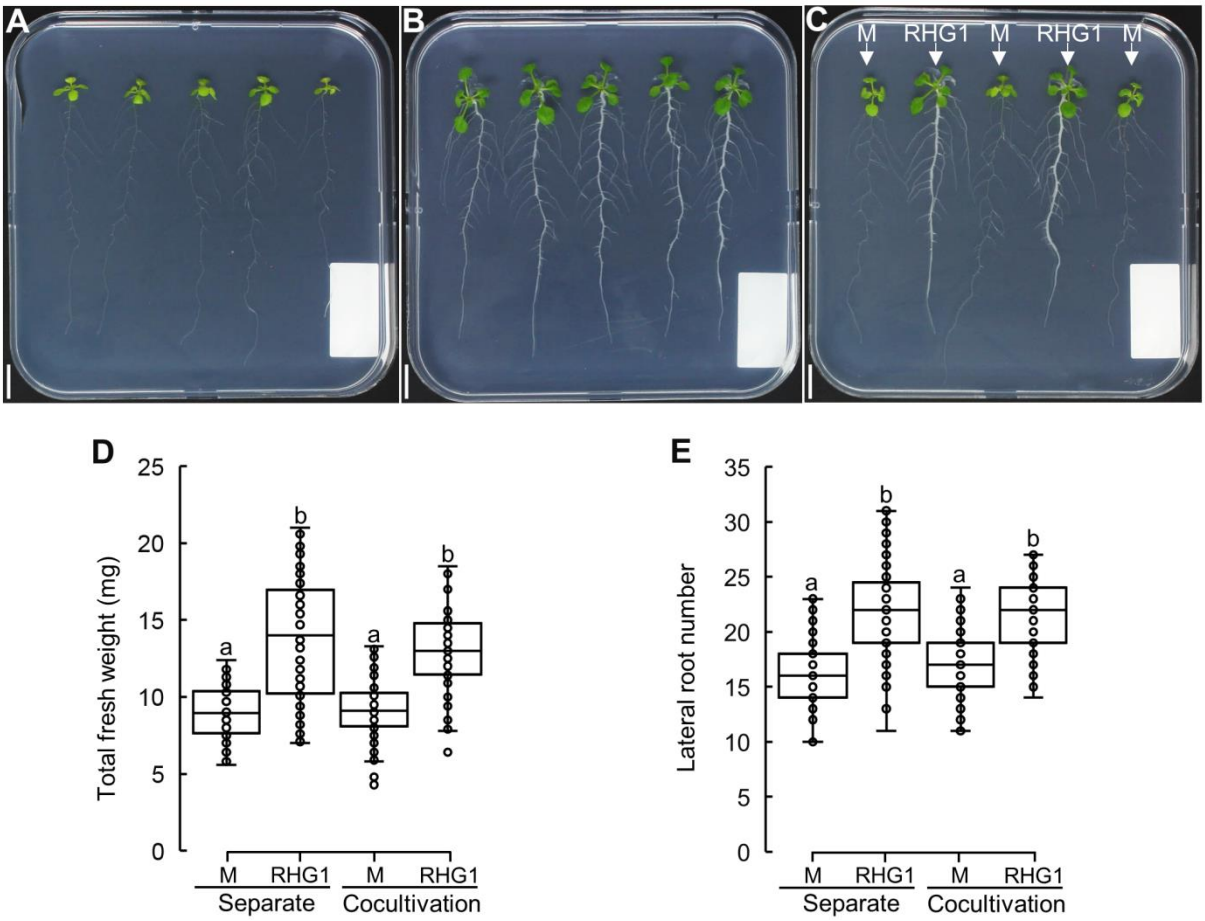

Supplementary Fig. 2. PGP effect of RHG1 in cocultivation *versus* separate setup. **A** and **B**, In the separate setup, the *Arabidopsis* seeds were mock-treated with PBS solution or inoculated with an RHG1 inoculum in different plates, respectively. **C,** In the cocultivation setup, the mock-treated and RHG1-inoculated seeds were placed next to each other in the same plates. Representative photographs of *Arabidopsis* seedlings at 14 DAIG are shown. Bar = 1 cm. **D and E**, Total fresh weight (**D**) and lateral root number (**E**) of mock-treated (M) or RHG1-inoculated (RHG1) plants grown in the separate or cocultivation setup determined at 14 DAIG. The boxplots present the combined data from three independent experiments with at least 20 plants per treatment in each experiment. Different letters indicate significantly different statistical groups ($P < 0.01$, Tukey's Honest Significance Difference test).

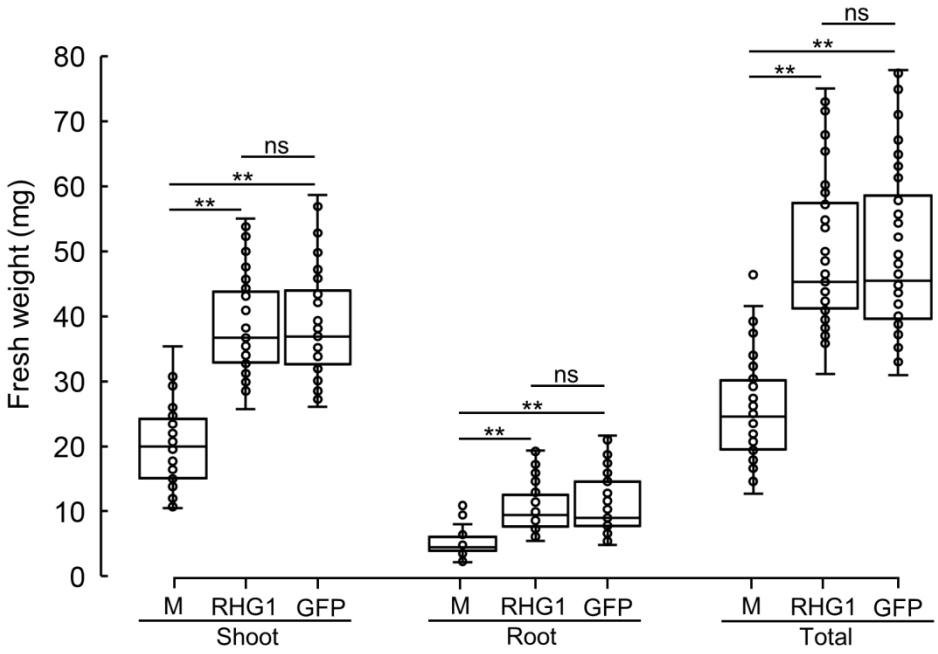

Supplementary Fig. 3. PGP effect of the GFP-labeled strain RHG1::GFP. *Arabidopsis* seeds were mock-treated (M) or inoculated with RHG1 (RHG1) or RHG1::GFP (GFP). The plant fresh weight was determined at 18 DAIG. The plot graphs were based on three biological replicate experiments ($n \geq 15$). Asterisks indicate significant differences between different treatments (** $P < 0.01$; ns, $P > 0.05$. Student's *t*-test).

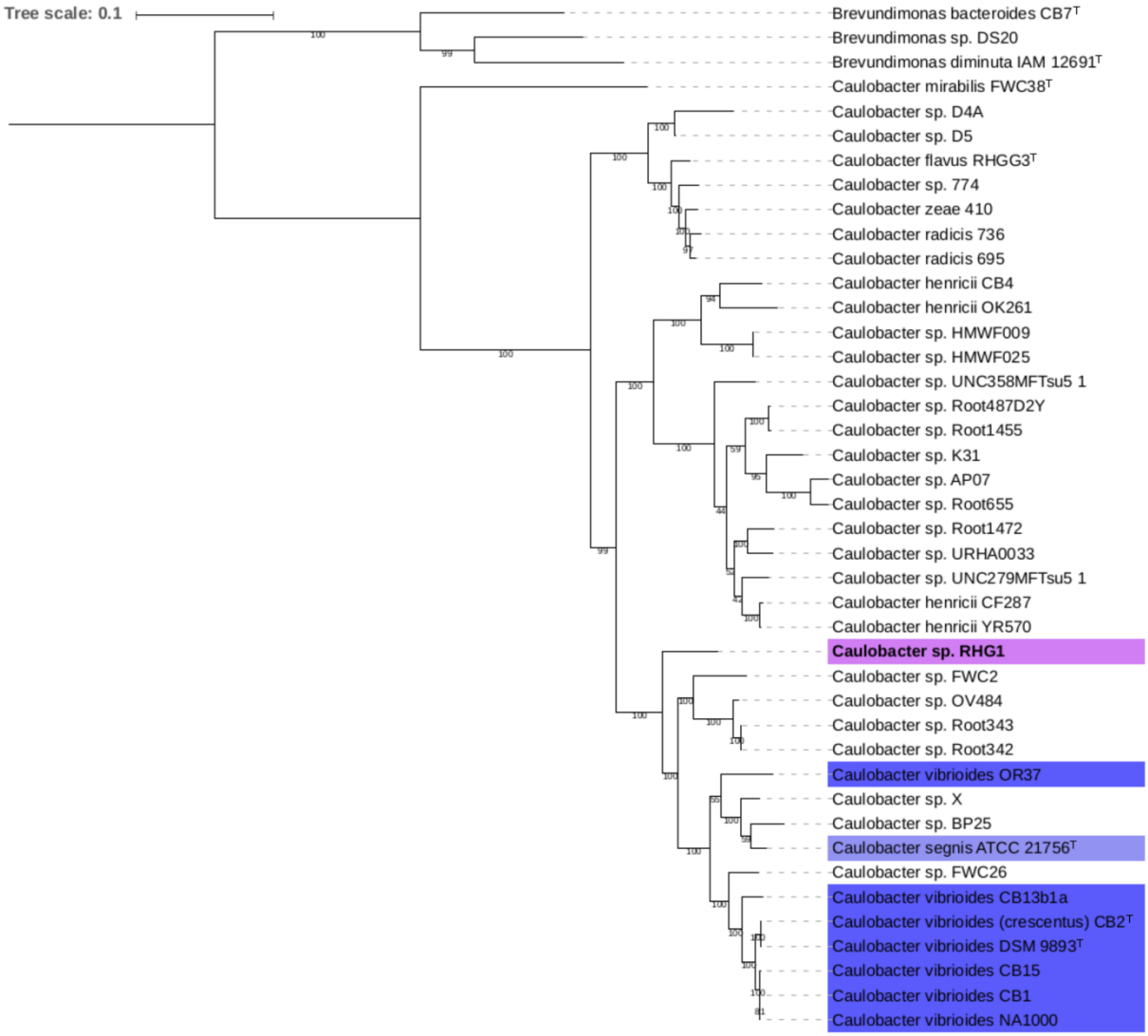

Supplementary Fig. 4. Phylogenomic tree showing the relationships of *C*. sp. RHG1 and other *Caulobacte*r species. The tree is based on the comparison of 107 essential core genes and constructed by means of the bcgTree software.

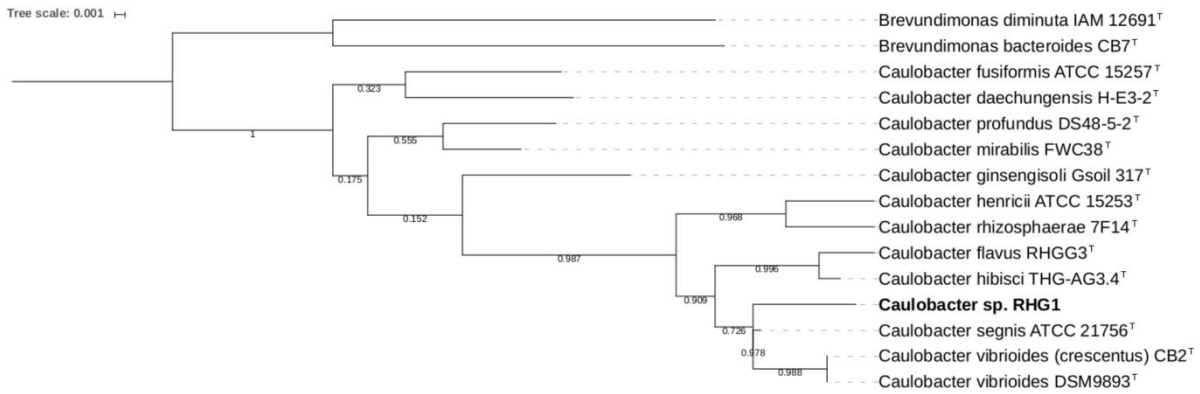

Supplementary Fig. 5. Phylogenetic tree obtained with the maximum likelihood method, based on the 16S rRNA genes of all the type strains inside the *Caulobacter* genus. The strains *Brevundimonas bacteroides* CB7 and *Brevundimonas diminuta* IAM 12691 were used as an outgroup.

Supplementary Fig. 6. Alignment of the NirK protein sequences from RHG1 (*Caulobacter*) with orthologs from *Azospirillum brasilense* Sp245, NirK1 (*Azospirillum*-1) and NirK2 (*Azospirillum*-2) (Pothier et al.,2008).

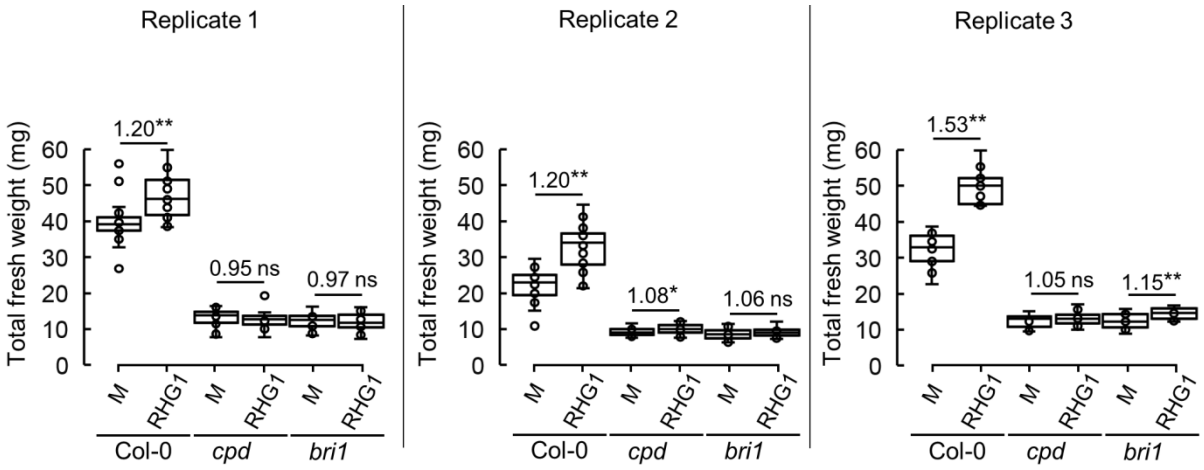

Supplementary Fig. 7. Effect of RHG1 on the plant fresh weight in Col-0, *cpd,* and *bri1.* Five-day-old seedlings were mock-treated (M) or inoculated with RHG1 (RHG1). Total fresh weight was determined at 14 DPI. Four independent replicates were performed ($n \geq 15$), of which the results are shown for three experiments (see Fig. 6 for the fourth). The value on top of the two boxes of each genotype indicates the fold change in weight between mock-treated (M) and RHG1-inoculated (RHG1) plants. Asterisks indicate significant differences between mock and inoculated plants (** $P < 0.01$; * $P < 0.05$; ns, $P > 0.05$. Student's *t*-test).